Amorphous metallic alloys

I. V. Zolotukhin and Yu. E. Kalinin

Voronezh Polytechnical Institute

Usp. Fiz. Nauk **160**, 75–110 (September 1990)

The experimental data on the structure of and the structural defects and structural relaxation in amorphous metallic alloys are reviewed. The elastic and inelastic properties of amorphous metallic alloys and the effect of disorder in the arrangement of atoms on the ferromagnetic properties of amorphous metallic alloys are also studied. Magnetoelastic phenomena are discussed in detail: the ΔE effect and magnetomechanical damping. Possible applications of amorphous metallic alloys in microelectronics, video recorders, and different types of transducers and sensors are discussed.

1. INTRODUCTION

Many scientists are now studying the structure and properties of disordered condensed media. The importance and necessity of studying such media are reflected in the following words of J. Ziman:[1] "This research is not purely academic: disordered phases of condensed matter—steel and glass, earth and water, if not fire and air—are far more abundant, and of no less technological value, than the idealized single crystals that used to be the sole object of study of 'solid-state physics'." Disordered condensed media include solids with glass-like structure, in particular, amorphous metallic alloys (AMAs), whose structure and properties are being studied intensively.

Why are amorphous metallic alloys interesting? First and foremost they are of interest because metallic alloys with short-range order in the arrangement of the atoms are very interesting objects and they expand our knowledge of the physics of condensed media. From the practical standpoint the increased interest in amorphous metallic alloys is due to the combination of unique physical properties found in them. Thus some amorphous metallic alloys consisting of ferromagnetic components are magnetically soft materials with better characteristics than permalloys, and at the same time they are mechanically strong, like very hard steels. The temperature coefficient of the electric resistance of amorphous metallic alloys can be close to zero in a wide range of temperatures, and the corrosion resistance of iron-based amorphous alloys with very small admixtures of chromium is significantly higher than that of stainless steel in the crystalline state.

Amorphous metallic layers were first produced by A. I. Shal'nikov more than 60 years ago. He used them for studying superconductivity in disordered structures.[2,3] Investigations of the structure of alloys formed under conditions of high rates of cooling were continued in the USSR at the beginning of the 1950s; this work resulted in the publication of the monograph of Ref. 4. However the tempo of research work on amorphous metallic alloys increased worldwide after the publication of the paper by Duwez *et al.*[5] A significant number of binary, ternary, and multicomponent systems of amorphous metallic alloys are now known. In the general case all amorphous metallic alloys are divided into two large groups: metal-metal and metal-metalloid. The first group consists of alloys of transition and precious metals (Fe, Co, Ni, Re, Ti, Pd, *et al.*) with metalloids (B, C, P, Si, Ge), whose atomic content is equal to 15%–20%. The second group consists of alloys of a) transition metals with one another (for example, Nb–Ni, Zr–Pd, etc.), b) simple metals with one another (Mg–Zn, Mg–Cu, etc.), c) simple metals with transition metals (Ti–Be, Zr–Be, etc.), d) simple metals with rare-earth metals (La–Al, La–Be, etc.), and e) transition metals with rare-earth metals (Gd–Co, Tb–Co, etc.). Aside from the binary alloys, the same elements can form numerous multicomponent amorphous alloys.

Progress in the technology of production of solids of this class has played a definite role in the increase in research work on amorphous metallic alloys. There are now a large number of different methods for producing alloys with amorphous structure. It is convenient to divide these methods into three large groups according to the starting aggregate state from which the amorphous metallic alloy is obtained: methods for producing alloys from gaseous, liquid, and solid crystalline states. The first group consists of the well-known methods of vacuum evaporation and condensation, cathodic sputtering, gas-thermal sputtering, etc. The second group consists of diverse methods of quenching from the liquid state, electrolytic and chemical deposition from the melt, laser-induced vitrification, etc. The third group consists of methods for transferring crystalline solids into an amorphous state by means of ion implantation and neutron irradiation, mechanical action and pressure, as well as activation of solid-phase reactions.

The purpose of this paper is to review briefly the present status of research on the structure of amorphous metallic alloys and its effect on some physical properties of these materials, to summarize the results of research on solids of this class, and to examine questions and problems which have not been studied.

2. THE STRUCTURE OF AMORPHOUS METALLIC ALLOYS

The spatial order in the arrangement of atoms in an amorphous structure is customarily called topological or configurational, while an ordered arrangement of atoms of different types in two-and many-component systems is customarily called chemical or compositional. The main "direct" methods for studying the structures of amorphous materials are diffraction of x-rays, electrons, and neutrons,[6,7] as well as the method of extended x-ray absorption fine structure (EXAFS).[8] The short-range order parameters (interatomic distance and coordination number) are determined by analyzing the radial distribution functions $4\pi r^2\rho(r)$ (RDFs) of the atoms. These functions are calculated by Fourier transforming the experimental data (here r is the distance and ρ is the density). Indirect methods, for exam-

 0038-5670/90/090720-19$01.00

ple, nuclear magnetic resonance, the Mössbauer effect, and others, are also used for analyzing the structure of amorphous metallic alloys.

In the study of amorphous structures there are definite difficulties in understanding and interpreting the experimental data, since the RDFs give only a one-dimensional representation of the real three-dimensional structure. This shortcoming makes it necessary to construct structural models and to compare the theoretical values of the parameters with the experimental values. However the choice of a model is also difficult, since all these models give the same structural parameters which makes it difficult to obtain an unequivocal interpretation of the topological arrangement of the atoms in an amorphous metallic alloy. Aside from the original experimental studies of the structure of amorphous metallic alloys a large number of reviews and monographs, concerning primarily diffraction methods of study[9-12] and modeling of the structure,[13-15] have now also been published. The experimental data are examined in detail in Ref. 9; we shall only briefly describe the main results.

1. The radial distribution functions of the atoms in an amorphous metallic alloy have several diffuse maxima. Characteristically the second peak is split into two peaks, one of which is stronger than the other, the ratios of the distances to the first peak being $r_2/r_1 = 1.63$–1.67 and $r_2'/r_1 = 1.87$–193. The first ratio is close to the average value for atoms occupying the vertices of two tetrahedra having a common base, while the ratio r_2'/r_1 approaches the distance $2d$ for three collinear atoms, where d is the diameter of an atom.

2. The ratio of the subpeaks of the split second peak depends on the composition of the alloy. For example, in the amorphous metallic alloy Fe–B the higher first subpeak becomes lower as the concentration of the metalloid increases. This indicates that the parameters of the short-range order in the system change as the content of the components changes.

3. For metal-metalloid systems the metal atoms are concentrated around the metalloid atoms.

2.1. Model representations of the structure of an amorphous metallic alloy

The existing methods for constructing models can be divided into three large groups according to the structural state of the starting material, i.e., gaseous, liquid, and solid. Models based on the construction of an amorphous structure from the solid crystalline and gaseous states are topological models in the form of polyhedra with atoms at the vertices. The first group of such models are "microcrystalline" models with short-range order characteristic for the corresponding crystal lattices. In the last few years the idea of the breakdown of long-range order as a result of special atomic coordination (Gaskell's model of coordination polyhedra[16,17]) or the introduction of a three-dimensional high-density network of dislocations and disclinations[18-20] has been introduced into the "microcrystalline" models.

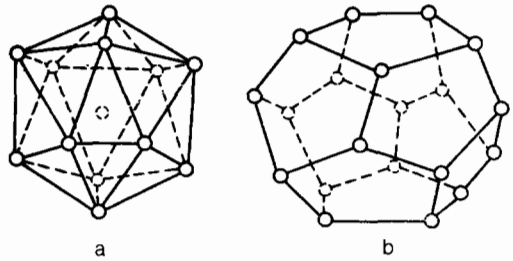

FIG. 1. Thirteen-atom icosahedron (a) and pentagonal dodecahedron (b).

The second group of topological models are "cluster" models, which are similar to the microcrystalline models, but the basic structural units are noncrystallographic ordered microclusters of atoms,[21,22] which play the same role as microcrystals. Figure 1 shows two possible structural units of this group:[21,23] a thirteen-atom icosahedron and a pentagonal dodecahedron—a so-called "amorphon," whose characteristic feature is a symmetry axis of fifth order. Interest in this group of models has increased in the last few years as a result of the discovery of a new class of materials—quasicrystals with icosahedral packing of the atoms.[24,25]

The third group of topological models of amorphous metallic alloys consists of models based on a combination of random close packings of rigid and soft spheres.[26-31] A version of the random packing of atoms as applied to covalent and oxide glasses is the model of a continuous random network.[32] All models of this group are characterized by a collection of spheres of the same size (or spheres of two sizes) packed randomly and relaxed to the highest density. They differ by the packing rules, the interaction potential, the method of relaxation, etc. In configurations of random, close packings the structural elements of both crystallographic and noncrystallographic packings can be distinguished. This can be seen clearly in the example of Bernal polyhedra (Fig. 2).[26]

Models based on the construction of a structure from the liquid state are constructed with the help of a computer by means of "rapid cooling" of the configurations characteristic of a liquid. In the process the analysis of the structure, in contrast to topological models, is usually conducted with the help of Voronoĭ polyhedra, in which the atoms occupy not the vertices, but rather sites inside the polyhedron. Nonetheless the form of this polyhedron preserves the characteristic symmetry elements in the arrangement of the atoms. A statistical-geometric analysis of the structure of amorphous metal-metalloid alloys showed[33] that the coordination around the metal atoms is represented by distorted icosahe-

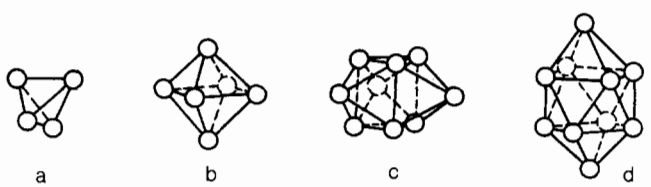

FIG. 2. Configuration of atoms in close packings according to Bernal. a) tetrahedron, b) octahedron, c) trigonal prism, d) Archimedean antiprism, e) tetragonal dodecahedron.

dra, while the coordination around the metalloid atoms is represented by the energetically most favorable structural forms (distorted octahedron, trigonal prism, or dodecadeltahedron). Generalized indices, making it possible to classify a structure with short-range order in the arrangement of the atoms, have been proposed for all Voronoĭ polyhedra.[34,35] The methods of modeling and models of the structure of amorphous alloys are examined in detail in the monographs of Refs. 14 and 15.

Analysis of the currently proposed structural models shows that they are in many ways similar. The similarity between the microcrystalline and cluster models lies in the assumption that there exist several structural units, whose topology, however, is different. In the case of the microcrystalline model these are crystallographic polyhedra, and in the case of the cluster model they are noncrystallographic icosahedra. The tetrahedral pore is also a common element for all topological models. Voronoĭ polyhedra, obtained by modeling by the method of molecular dynamics from the liquid state, also consist of distorted polyhedra, similar to some topological models, and reflect their symmetry. This similarity and the presence of fifth-order axes in the amorphous structure indicate that on the whole our understanding of the general characteristics of the packing of atoms in amorphous metallic alloys is correct, and the proposed models give a relatively good approximation to the real structure, since they reproduce some parameters quite well, for example, many features of the experimental radial distribution functions. In addition, with the help of cluster and close-packing models it is possible to explain the variation in many structurally sensitive properties. At the same time, it should be noted that amorphous metallic alloys are, as a rule, diverse and have many components, and the structural models sometimes give a far from adequate representation of the real structure. At the present time there does not exist a universal model of the noncrystalline state that is suitable for arbitrary systems and that permits describing the structure adequately and relating the structure with the properties.[36] Such a universal model apparently does not exist, since the noncrystalline state is more diverse than the crystalline state. There exists such a multitude of structures with different short-range order that it is hardly possible to describe the order with a universal model. Apparently, it is necessary to use a model with the short-range order appropriate to the case at hand. Moreover, since amorphous metallic alloys are multicomponent materials, the model must be heterogeneous, i.e., each constituent atom of the structure must have its own short-range order. In conclusion we note that in the case when real crystals are being modeled the ideal structural models are supplemented by defects in the crystal lattice, which play an important role in the interpretation of many physical properties. This analogy apparently should be preserved also in the modeling of the structure of amorphous metallic alloys.

2.2. Structural defects in amorphous metallic alloys

The study of the properties of amorphous metallic alloys shows that they are structurally sensitive to and depend on the conditions under which the alloys were prepared, the conditions of heat treatment, and other external actions. This is indicated by investigations of structural relaxation in amorphous metallic alloys, as a result of which the structural changes at temperatures which do not lead to crystallization give rise to changes in the mechanical, electric, magnetic, and other properties.[37] By analogy to crystals the structurally sensitive properties of amorphous metallic alloys are also determined by defects in the amorphous structure.

The separation of the entire structure of an amorphous solid into defect-free (ideal) and defective is important not only from the theoretical standpoint, but also from the practical standpoint. Since amorphous bodies do not have long-range order in the arrangement of the atoms, in the presence of short-range order it must apparently be recognized that in the "ideal" amorphous structure there are no disruptions of the short-range order.[38,39] If there are disruptions in the short-range order, then these disruptions will be defects of the amorphous state.

Structural defects on an atomic scale (< 1 nm) are usually regarded as point defects. These defects are considered to be fluctuations of the free volume,[40] vacancies and pseudovacancies,[41,42] n-, p-, and τ-defects,[43-45] and other types of defects.[46] Thus a defect of the p-type is a section of high local density of the amorphous structure, while defects of the n-type are a local fluctuation of low density, corresponding to excess free volume. Fluctuations of the shear stresses—τ-defects—are also introduced as characteristics of shear stresses. The definition of point defects that is connected with the perturbation of the coordination number deserves attention.[38] Since amorphous bodies are characterized by the presence of short-range order, one characteristic of which is the coordination number, the structure in which the coordination of a given type of atom is conserved is ideal, while local sections whose coordination is different from the normal coordination will represent structural defects. The simplest defect in this definition is one in which only one atom has a coordination differing by one unit from the ideal coordination, i.e., from the coordination Z characteristic for the "ideal" state. Defects of the vacancy type can be represented as a collection of Z of the simplest defects with coordination $Z - 1$ for the surrounding atoms and a defect of the type of an interstitial atom can be represented as a collection of Z of the simplest defects with the coordination $Z + 1$. Thus the simplest defects can exist only in amorphous structures, and their different combinations with one another generate a great variety of complex point defects. We note that point defects of the type of a vacancy or an interstitial atom in a crystal lattice comprise a definite collection of elementary defects arranged in an ordered fashion. With this definition of defects some cells in Bernal's model (3–5 in Fig. 2) will be defects of the amorphous structure, since when the space is filled with such polyhedra the coordination number of some atoms will be less than the ideal coordination.

Structural fluctuations at the microscopic level (10–100 nm) are ascribed to the existence of "quasidislocation dipoles"[47] and linear disclinations.[48] Thus if it is assumed that the main structural elements of amorphous metallic alloys are 13-atom icosahedra (see Fig. 1a), then the distortion-free regular icosahedral packing (defect-free glass) can be realized only in a space of constant curvature, for example, in a three-dimensional sphere S^3. In order to transfer a defect-free amorphous metallic alloy into the flat space R^3 disclinations must be introduced into the structure of the alloy.[48-50] The nuclei of such disclinations consist of clusters

whose symmetry differs from the icosahedral symmetry.

Diffraction investigations in some amorphous metallic alloys have revealed structural components that are distinguished by the type of short-range order[51,52] and are characterized by phase separation. To study such structures it is necessary to introduce interphase boundaries, which are defects of the planar type.

Thus the question of the classification of structures of short-range order and their disruptions (structural defects) is open and requires further study.

2.3. Structural relaxation

Investigations of the structural state of amorphous solids have shown that irrespective of the method of preparation an amorphous metallic alloy is not in a state of metastable equilibrium. The transition into a state of metastable equilibrium, characteristic for a given amorphous system under definite external conditions, is accompanied by a change in the physical properties. For example, on heating or isothermal annealing below the vitrification point (i.e., the temperature at which the liquid melt freezes) the density increases, the elastic modulus increases, the diffusion coefficient decreases, etc.[37] The change in these and other properties is connected with the process of structural relaxation, when the frozen amorphous structure relaxes to a state of metastable equilibrium.[53] In the process of structural relaxation there occur atomic displacements that lead to changes[54] in a) the interatomic distance between the nearest neighbors, b) the average interatomic distance, and c) the average chemical order. Based on the x-ray diffraction data on structural changes accompanying relaxation in the amorphous alloy $Fe_{40}Ni_{40}P_{14}B_6$ Egami[45] concluded that as a result of structural relaxation the peaks in the structure factor curves become higher and narrower. The relative changes in the height of the first and second peaks are of the order of 2%–3%, but the change in the shoulder of the second peak and the change in the maxima from the third to the fifth peak are equal to approximately 10%. Structural relaxation is also caused by the motion of many atoms, resulting in ordering of the nearest-neighbor atoms around the chosen atom. Similar results have also been obtained for other amorphous metallic alloys.[55,56]

For the case of amorphous metallic alloys obtained by quenching from the liquid state structural relaxation can be interpreted based on the scheme of Fig. 3 which presents the dependence of the free energy F on the temperature T and the volume V, which appears as a structural parameter of the condensed state of the material.[57] The dependence of the free energy on the structural parameter V has the form of a potential well for both the solid crystalline state F_S and the liquid state F_L. This character of the dependence of the free energy on the structural parameter results from the fact that in the state of equilibrium the free energy of the system is minimum. For example, the elastic part of the free energy of a solid U can be represented as a quadratic function of the change in volume:[58]

$$U(V) - U(V_0) = \frac{1}{2} K (V - V_0)^2 V_0^{-1}; \qquad (2.1)$$

here V_0 is the equilibrium volume and K is the compression modulus.

At temperatures above the melting point T_m the bottom

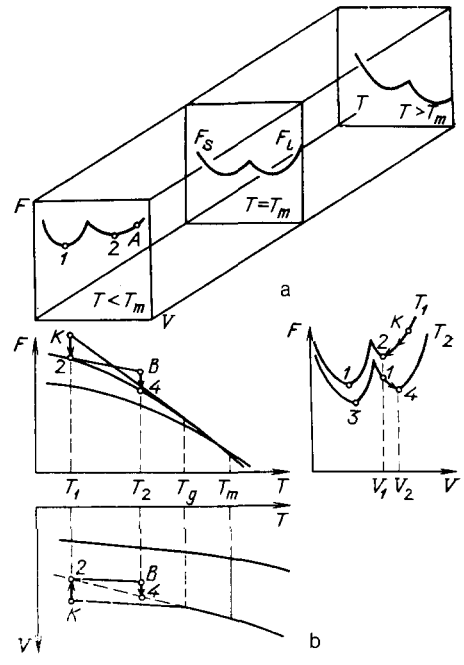

FIG. 3. The free energy of the condensed state as a function of the temperature and volume.

of the potential well F is lower for the liquid state, while at temperatures below T_m it is lower for the solid crystalline state. By rapid quenching from the liquid state it is possible to achieve a situation in which at low temperatures the system remains in the metastable state characteristic for a supercooled liquid (the point 2 at $T < T_m$ in Fig. 3a). At temperatures below the vitrification point (T_g) the structure freezes and the system is now characterized by the point A (Fig. 3, $T < T_m$). Such a state is a nonequilibrium state, not only with respect to the stable crystalline equilibrium, but also with respect to the metastable equilibrium, characteristic for a supercooled liquid. The process of relaxation of the amorphous structure from the nonequilibrium state (the point A at $T < T_m$ in Fig. 3a) into a state of metastable equilibrium (the point 2 at temperatures $T < T_m$ in Fig. 3a) is customarily called structural relaxation, in contrast to the crystallization process, which is associated with a transition into a state with an absolute minimum of the free energy (the point 1 in Fig. 3a). In accordance with what was said above, the free energy as a function of the temperature and volume is described by the relation

$$dF = \left(\frac{\partial F}{\partial T}\right)_V dT + \left(\frac{\partial F}{\partial V}\right)_T dV; \qquad (2.2)$$

whence

$$\frac{dF}{dT} = \left(\frac{\partial F}{\partial T}\right)_V + \left(\frac{\partial F}{dV}\right)_T \frac{dV}{dT}. \qquad (2.3)$$

It follows from this expression that in the general case the temperature coefficient of the free energy F is determined by the temperature coefficient $(\partial F/\partial T)_V$ and some quantity equal to the thermal coefficient of the volume change dV/dT multiplied by a factor that depends on the structure of $(\partial F/\partial V)_T$. Therefore the physical properties of amorphous metallic alloys will depend strongly on the structure and will change when the structural parameter changes.

The change in the structural parameter V with the temperature for the equilibrium crystalline and metastable states is connected with, on the one hand, the anharmonicity of the vibrations of the atoms and, on the other, the change in the equilibrium concentration of defective configurations of the vacancy type. Taking into account the fact that below the vitrification point (T_g) the structure freezes, the concentration of defective configurations of the ith type C_i and the associated excess free volume for amorphous and supercooled states can be expressed as [59]

$$\begin{aligned} C_i &= C_0 \quad \text{for } T < T_g \\ &= Ae^{-U_i/kT} \quad \text{for } T_g < T < T_x \end{aligned} \tag{2.4}$$

where C_0 is a constant, equal to the equilibrium concentration of defects for $T = T_g$; U_i is the formation energy of the ith defect; k is the Boltzmann's constant; and, T_x is the crystallization temperature. Thus below the vitrification point a nonequilibrium concentration of defective configurations obtains and it can change as a result of structural relaxation.

As possible mechanisms of structural relaxation, models have been proposed according to which the freshly quenched amorphous metallic alloy can be represented as consisting of distorted, randomly packed, trigonal prisms, which relax to a closer packed structure of undistorted trigonal prisms[60] or consist of complexes of icosahedra which transform into isolated and more regularly packed icosahedra.[56] Computer modeling[45] shows that the irreversible part of the relaxation could be due to the annihilation of positive and negative fluctuations of the free volume. It can also be conjectured that the process of structural relaxation is determined by a decrease in the concentration of frozen defective configurations of the vacancy type to a value characteristic for the metastable state at the given temperature. This process requires that the immediate atomic environment be restructured, i.e., it is an activational process and proceeds more rapidly at temperatures close to the vitrification point. If the amorphous structure is represented as a collection of tetrahedra (the basic structural units) and polyhedra with a large number of atoms at the vertices (defects of the amorphous structure),[61] then the structural relaxation can be connected with irreversible changes of the defective configurations and the associated decrease of their free volume.

The rate at which the nonequilibrium amorphous structure approaches the metastable equilibrium at a definite temperature $T_1 < T_g$ can be assumed to be proportional to the degree of departure from equilibrium. If the difference $V - V_0$, where V and V_0 are the values of the structural parameter for the amorphous structure and the metastable state at the temperature T_1, respectively, is used as a measure of the degree of departure from equilibrium, then

$$\frac{d(V-V_0)}{dt} = -\frac{1}{\tau}(V-V_0), \tag{2.5}$$

where τ is the relaxation time characterizing the mobility of the structural defects, whose diffusion determines the convergence of the amorphous alloy to a state of metastable equilibrium;

$$\frac{V(t)-V_0}{V(0)-V_0} = e^{-t/\tau}. \tag{2.6}$$

For quantitative calculations of the stabilization of the properties of amorphous metallic alloys it is necessary to take into account the temperature dependence of the relaxation time

$$\tau = \tau_0 e^{-U(V)/kT} \tag{2.7}$$

and the existence of a distribution of defects in the structure. As a result Eq. (2.6) becomes

$$\frac{V(t)-V_0}{V(0)-V_0} = \int_0^\infty Q(\tau)\, e^{-t/\tau} d\tau, \tag{2.8}$$

where $Q(\tau)$ is a distribution function, satisfying the normalization condition

$$\int_0^\infty Q(\tau)\, d\tau = 1.$$

In practice the kinetics of structural relaxation is also analyzed with the help of the empirical relation[12]

$$\frac{P(t)-P_\infty}{P(0)-P_\infty} = \exp\left[-\left(\frac{t}{\tau}\right)^n\right], \tag{2.9}$$

where $P(t)$, $P(0)$, and P_∞ are the values of the parameters at $t = t$, 0, and ∞, respectively, and $0 < n < 1$.

In cyclical regimes of heat treatment of amorphous metallic alloys reversible changes are observed in many physical properties.[62-64] This is connected with the so-called "reversible" structural relaxation. Such structural changes can be understood by appealing once again to the scheme shown in Fig. 3b, where the dependence $F(T,V)$ (see Fig. 3a) is shown in the form of two projections $F(V)$, $V(T)$ and two sections $F(V)$ at the temperatures T_1 and T_2. After prolonged annealing at the temperature T_1 the system with the amorphous structure relaxes from the nonequilibrium state corresponding to the point K into its own metastable state characterized by a minimum of the free energy (point *2* in Fig. 3b). This state is characterized by a definite concentration of structural defects or by the structural parameter V_1. When the material is heated up to a temperature T_2 below the vitrification point T_g because of the long relaxation times the system once again leaves its metastable equilibrium state since at the given temperature there is a unique concentration of equilibrium defects or a unique structural parameter V_2, which is now characterized by the point B in Fig. 3b. In the case of isothermal annealing, i.e., under conditions when the temperature T_2 is maintained constant, the system will relax with the thermodynamic potential decreasing from the point B into a state of metastable equilibrium characterized by the point *4*. However this process is now different from the structural-relaxation process occurring at $T = T_1$. At $T = T_1$ structural relaxation occurs with a decrease of the structural parameter V, whereas at $T = T_2$ structural relaxation occurs with an increase in V. This process, resulting in an increase of the concentration of defective configurations and therefore in reversible restoration of the structure (or V), is customarily regarded as reversible structural relaxation.

Thus the change brought about in the physical properties of amorphous metallic alloys by a change in the structure as a result of structural relaxation can be uniquely attributed to the presence of defects of different types in the structure of the alloys. The deviation of the structure of amorphic metallic alloys from the metastable equilibrium when the alloys are cooled is caused by freezing of some

concentration of defective configurations. From this viewpoint the vitrification temperature is the temperature at which the concentration of frozen defects becomes equal to the equilibrium concentration, i.e., the vitrification temperature is analogous to the temperature of freezing of vacancies in a crystal when the crystal is cooled. In many cases, however, structural relaxation is accompanied by diffusive redistribution of the constituent elements of the alloy, i.e., phase separation. Thus Mössbauer spectroscopy revealed that in the amorphous alloy $Fe_{40}Ni_{40}P_{14}B_6$ the initial homogeneous amorphous matrix decomposes as a result of heat treatment and forms two of the most probable types of nearest-neighbor atomic environments which are ordered in accordance with the stoichiometry of the crystalline phases of this alloy.[65] Here it is desirable to study experimentally and theoretically the amorphous structure of different types of short-range order and defects of definite type as well as to investigate their effect on the physical properties. From this standpoint it would be useful to perform experiments on the effect of different types of actions (irradiation, plastic strain, thermal and thermomagnetic annealing, etc.) on the structure and properties as well as to perform computer modeling by the method of molecular dynamics for the purpose of determining the structural configurations and their distribution in "quenched" and "heat-treated" amorphous structures.

3. ELASTIC AND INELASTIC PROPERTIES

3.1. Elastic properties of amorphous metallic alloys

For amorphous metallic alloys, just as for crystalline solids, for small strains Hooke's law is satisfied

$$\sigma_{kl} = C_{klmn}\varepsilon_{mn}, \tag{3.1}$$

where σ_{kl} are the components of the stresses, ε_{mn} are the components of the strains, and C_{klmn} are the stiffness constants. Of the 81 elastic stiffness coefficients, in the case of cubic crystals three are independent. The elastic constants in this case can be represented in the form of a symmetric matrix[13]

$$C_{\alpha\beta} = \begin{vmatrix} C_{11} & C_{12} & C_{12} & 0 & 0 & 0 \\ C_{12} & C_{11} & C_{12} & 0 & 0 & 0 \\ C_{12} & C_{12} & C_{11} & 0 & 0 & 0 \\ 0 & 0 & 0 & C_{44} & 0 & 0 \\ 0 & 0 & 0 & 0 & C_{44} & 0 \\ 0 & 0 & 0 & 0 & 0 & C_{44} \end{vmatrix} \tag{3.2}$$

The indices α and β taking on values from 1 to 3 correspond to the normal components of the stress and strain while the indices for values from 4 to 6 correspond to the shear components. For amorphous bodies, which are usually completely isotropic (with the exception of magnetostriction alloys), the matrix (3.2) has the same from, but the number of independent constants is reduced to two as a result of the additional equation

$$C_{11} = C_{12} + C_{44}. \tag{3.3}$$

The shear modulus G and the bulk modulus K can be chosen as the independent constants. They are related with the components of the matrix (3.2) by the expressions

$$G = C_{44}, \tag{3.4}$$

$$K = \frac{1}{3}(C_{11} + 2C_{12}). \tag{3.5}$$

The relation between these moduli, Poisson's ratio ν, and Young's modulus E is determined by the expressions

$$E = 3(1 - \nu)G, \tag{3.6}$$

$$K = \frac{E}{3}(1 - 2\nu). \tag{3.7}$$

Table I gives experimental data, obtained with the help of resonance, ultrasonic, and static methods, on the elastic properties of some amorphous alloys.

In all cases the elastic moduli of the amorphous alloys are lower than the analogous moduli of the corresponding crystalline analogs or the crystalline metals on which the corresponding alloy is based. This behavior is associated with the presence of excess free volume and reflects the fact that in the amorphous state the average interatomic interaction force is weaker than in crystals. Structural relaxation resulting in a decrease of the excess free volume gives rise to an increase in the elastic moduli of the nonmagnetostriction amorphous alloys by several percent.[69]

Aside from the excess free volume, the strength and character of the chemical bonds, which depend on the composition of the alloy, significantly affect the value of the elastic moduli. Increasing the content of metalloid atoms increases Young's modulus from 158 to 187 GPa in the alloys Fe–Si–B, from 150 to 152 GPa in the alloys Fe–P–C, and from 173 to 175 GPa in the alloys Co–Si–B.[70] In addition, there exists a correlation between Young's modulus, the microhardness, and the ultimate strength. All this indicates that the mechanical behavior of amorphous metal alloys is

TABLE I. The elastic characteristics of some amorphous (A) and crystalline (C) alloys at room temperature.

Alloy	Structure	E, GPa	G, GPa	K, GPa	ν	References
$Pd_{77,5}Cu_6Si_{16,5}$	A	98,1	34,8	182,0	0,41	[66]
	K	130,0	46,9	194,0	0,385	[66]
Sm_2Co_{17}	A	131,2	39,4	130,2	0,332	[37]
	K	181,8	57,9	140,0	0,283	[37]
$Pd_{80}Si_{20}$	A	68	35	182	0,4	[11]
$Cu_{50}Zr_{50}$	A	85,1	31,1	104,2	0,364	[37]
SiO_2	A	76	31	37	0,17	[67]
$Fe_{40}Co_{40}B_{20}$	A	166	61	206	0,365	[13]
$Pd_{80}P_{20}$	A	80,5	28,6	144,2	0,407	[68]
$Pt_{75}P_{25}$	A	93,4	32,7	207	0,425	[68]
$Co_{75}B_{25}$	A	179,4	67	183,4	0,337	[68]

TABLE II. The basic characteristics of relaxational processes observed in amorphous metallic alloys.

Alloy	Temperature of peak, K	τ_0, s	E, eV	References
$La_{80}Al_{20}$	190	$3\cdot10^{-14}$	0,4	[71]
$La_{75}Al_{25}$	220	$3\cdot10^{-14}$	0,44	[71]
$Cu_{50}Zr_{50}$	314	$1,4\cdot10^{-14}$	0,69	[72]
$Co_{35}Y_{65}$	260	$2,2\cdot10^{-14}$	0,56	[72]
$Co_{35}Dy_{65}$	262	$7,7\cdot10^{-15}$	0,59	[72]
$Fe_{32}Ni_{36}Cr_{14}P_{12}B_6$	246	—	1,08	[73]
$Fe_{40}Ni_{40}P_{14}B_6$	258	—	1,48	[73]
$Co_{89}Tb_{11}$	488	$1\cdot10^{-13}$	0,8	[74]
Nb_3Ge	260	$2\cdot10^{-13}$	0,52	[75]
$Pb_{80}Si_{20}$ (H)	180	$1,4\cdot10^{-14}$	0,33	[76]
$Pd_{77,5}Cu_6Si_{16,5}$ (H)	160	$3\cdot10^{-13}$	0,31	[77]
$Nb_{40}Ni_{60}$ (H)	230	$3\cdot10^{-14}$	0,47	[78]
$Pd_{77,5}Cu_6Si_{16,5}$	250	$1\cdot10^{-13}$	0,52	[79]
$Cu_{50}Ti_{50}$	270	—	—	[80]

similar to that of crystalline metal alloys. On the other hand, the ratio of the ultimate strength to Young's modulus for amorphous alloys is $\sigma/E = 0.02$–0.03, which is almost one-half the value $\sigma/E = 0.05$ corresponding to the theoretical strength.[11] This value is much higher than the known value for most of the strong crystalline materials now employed ($\sigma/E = 10^{-5} - 10^{-2}$). This result indicates that in amorphous alloys linear structural defects, analogous to dislocations of the crystal lattice and responsible for plastic strain, are either absent in the starting state or are strongly pinned owing to the high concentration of defects giving rise to high internal stresses. Further investigations should give a more accurate answer.

3.2. Inelastic properties of amorphous metallic alloys

In amorphous metallic alloys, as in crystalline metals and alloys, a number of deviations from the purely elastic behavior, which have been termed inelastic phenomena, are observed in the region of elastic strains where Hooke's law operates. Inelastic effects, observed at low stresses, are the main reason for the internal friction (IF), which characterizes the irreversible energy losses within a solid in the process of mechanical vibrations.

The experimental data obtained from the study of internal friction showed that for many amorphous metallic alloys attenuation maxima of the relaxation type, whose height and position depend on the composition of the alloy and the structural state of the material, are observed in the temperature dependence of the internal friction in the temperature range $T = 200$–400 K. Table II shows the basic characteristics of the relaxation maxima studied for some amorphous alloys as well as maxima owing to the presence of hydrogen in the amorphous structure.

The tabulated data can be supplemented by some characteristic features of the relaxational maxima:

1. The peak is two to three times higher than the Debye peak, corresponding to a single relaxation time.

2. Plastic prestraining (for small strains) increases the degree of relaxation, and increasing the annealing temperature and time decreases the height of the maximum and shifts it into the region of high temperatures.

3. The characteristic relaxation time is $\tau_0 \sim 10^{-13} - 10^{-14}$ s.

The existence of peaks of the internal friction for many amorphous metallic alloys is proof of the existence of atomic configurations with short-range order which differ from the average configurations (defects of the amorphous structure) and which create a response to external mechanical stresses by means of local rearrangement of the atoms. The elementary acts of such rearrangement are atomic hops; this is indicated by the characteristic time $\tau_0 \sim 10^{-13}$ s. The fact that the relaxation peaks are two to three times wider than the Debye peak indicates that there is a spread in the parameters of fixed atomic configuration as a function of the energy; this is a consequence of the fact that there is size distribution of "point-like" defects (see Sec. 2). Heat treatment reduces the height of the internal-friction peaks;[81] this is connected with structural relaxation and decrease in the concentration of defective configurations.

At higher temperatures (from temperatures 150–200 K below T_g and higher) exponential growth of the attenuation of mechanical oscillations is observed;[82–87] this is the high-temperature background. Figure 4 shows the typical temperature dependence of the internal friction of the amorphous alloy $Pd_{40}Ni_{40}P_{20}$.[88] Two sections of exponential growth can be distinguished on it: from 360 K up to the vitrification point T_g and from T_g up to T_x. The sharp drop in the internal friction at higher temperatures is associated with the crystallization of the amorphous phase. It should be noted that the process of crystallization of amorphous metallic alloys having a complex composition is accompanied by the appearance of not one but several peaks of the internal friction.[89] These peaks appear as a result of the multistage nature of the crystallization process, i.e., transitions through a series of metastable states.

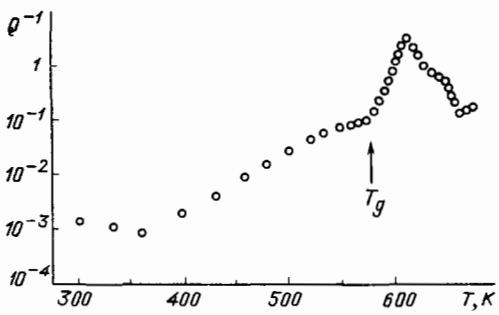

FIG. 4. The temperature dependence of the internal friction of the amorphous alloy $Fe_{40}Ni_{40}P_{20}$ for a heating rate of 0.85 K/min.

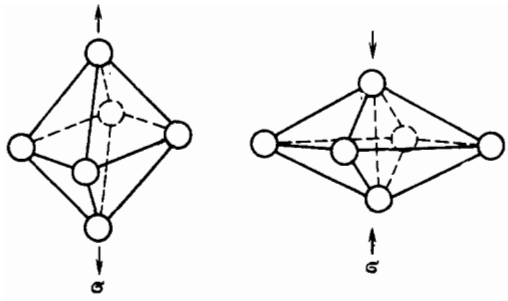

FIG. 5. The change produced in the structural configurations of an amorphous metallic alloy by external mechanical stresses.

Analysis of the data on the frequency dependence of the high-temperature background of the internal friction of amorphous metallic alloys at temperatures $T < T_x$ shows that its magnitude reaches maximum values at low frequencies and decreases as the frequency of the mechanical oscillations increases. This dependence is characteristic also for inorganic glasses.[90] A configurational model, which explains the appearance of the high-temperature background, was proposed in Ref. 63 based on the experimental data of Refs. 91–93. It is believed that the relaxation processes are caused by the transformation of some structural units into other structural units (Fig. 5).

The explanation given in Ref. 59 is perhaps more realistic. According to this explanation the exponential growth of the internal friction in the first (low-temperature) section is connected with migration of mobile structural units (defects), whose concentration is constant and which form when the amorphous state is obtained, under the action of mechanical stresses, while in the second section (high-temperature) it is caused by the migration of structural units formed in the process of thermal activation. The internal friction is estimated by the expression

$$Q^{-1} = \frac{CVG\varepsilon^2\nu_0}{\omega kT} e^{-U/kT}, \tag{3.8}$$

where C is the concentration of defects, V is the size of a defect, G is the shear modulus, ε is the magnitude of the elastic strain, ν_0 is the characteristic relaxation rate, ω is the frequency of the mechanical vibrations, k is Boltzmann's constant, and U is the activation energy of migration of a defect. Since the size of the defects and the activation energy for their migration in amorphous metallic alloys have a wide spread, it is difficult to draw a reliable conclusion about the nature of the migrating defects from the experimental data. The activation energy U, determined experimentally based on the formula (3.8), is an effective energy, since it does not take into account the distribution of τ and U. Analysis of the high-temperature background internal friction with the help of the continuous spectrum of relaxation times shows[94] that in this case it is necessary to use a wide distribution of relaxation times τ, which, in its turn, is determined by the wide spectrum of activation energies. Thus, if the activation energy is estimated with the help of the expression

$$\frac{U}{T} = k \ln(\omega\tau_0), \tag{3.9}$$

where $\tau_0 = 10^{-13}$ s, then depending on the temperature the values of U for the amorphous alloy $Fe_{32}Ni_{36}Cr_{14}P_{12}B_6$ range from 1.2 to 1.7 eV.[63] Analogous results are also obtained when U is determined from the temperature displacement of the internal-friction background when the frequency is varied.

Thermal annealing at temperatures which do not lead to crystallization of the alloy reduces the internal-friction background and shifts the start of the exponential growth of the internal-friction curve toward higher temperatures.[91,95] In addition, in the annealing process, a unique metastable state is achieved owing to structural relaxation, and this gives a definite attenuation. However annealing at a high temperature after prolonged annealing at a low temperature increases the internal-friction background; this is explained by the process of "reversible" structural relaxation (see Sec. 2).

Thus high-temperature investigations of internal friction yield information about the kinetics of defects in the amorphous structure. However the question of the nature of the defects responsible for the appearance of the internal-friction background in amorphous metallic alloys remains open, since it has not been solved even for the simplest systems in the crystalline state. To elucidate these questions as well as to determine more accurately the spectra of the distribution of the activation energies and relaxation times it is necessary to perform further investigations at different frequencies and amplitudes of deformation; this will yield additional information about the behavior of defects in amorphous metallic alloys.

The results of the study of the amplitude dependence of the attenuation of elastic oscillations in amorphous metallic alloys are of special interest. In crystalline materials such data make it possible to elucidate the mechanism of hysteretic internal friction, determined by dislocations.[96,97] A few numerical investigations of the amplitude dependences of the internal friction in amorphous metallic alloys have shown[79,80,98] that the character of the internal friction changes substantially after plastic prestraining.

4. MAGNETIC PROPERTIES

4.1. Effect of the disordered arrangement of atoms on the ferromagnetic properties

The fundamental possibility of the existence of amorphous ferromagnets was first pointed out by A. I. Gubanov in 1960.[99] Experimental proof of the existence of ferromagnetism in an amorphous film of iron was presented in 1964.[100] Since then interest in understanding the fundamental reasons for magnetism in amorphous alloys has not flagged. There is a large number of reviews and monographs devoted to the magnetic properties of amorphous metallic alloys,[11–13,101] so that we shall discuss only some aspects to which earlier less attention was devoted.

The first question that must be answered is: how does the magnetic moment of an atom of a ferromagnet change in the presence of long-range order in the arrangement of the atoms? We shall bear in mind the fact that magnetism in crystalline alloys consisting of transition metals is predominantly a local phenomenon, determined by the average environment of the atoms having magnetic moments. For this reason, models of the local environment,[102,103] largely determined by the chemical short-range order (CSRO), are employed to explain magnetism in structures with short-range

order. According to Ref. 104 four aspects of CSRO are important for magnetism: the number, type, distance, and symmetry of the nearest neighbors around a fixed position of the magnetic atom. All this can be expressed quite simply in terms of the molecular field for the Curie temperature

$$T_c = J(r) ZS(S+1)(3k)^{-1} \tag{4.1}$$

or Stoner's criterion, which determines the condition for the existence of a local moment:

$$J(F)N(F) > 1; \tag{4.2}$$

here $J(r)$ is the interatomic exchange integral, which depends on the distance; Z is the coordination number of an atom with a distinct magnetic moment; S is the spin quantum number; k is Boltzmann's constant; $J(F)$ is Stoner's integral, calculated at the Fermi level and reflecting the interatomic exchange interaction (Hund's rule); and, $N(F)$ is the electron density of states at the Fermi level. $N(F)$ is averaged at some site and J is a function of these states, localized around an atom. The number, type, and distance to the nearest neighbors are determined in terms of Z and $J(r)$ as well as in terms of $N(F)$ and $J(F)$. The symmetry in the arrangement of the nearest neighbors affects $N(F)$ and $J(F)$ and changes the distribution of the electronic states. Thus the formation of a local magnetic moment is determined by the space in which the intra-atomic exchange is realized quite freely.

We shall examine the existing ideas about the effect of disordering on magnetism. It is known[105] that antiferromagnetic compounds became ferromagnets with a transition into the amorphous state. Such a transformation can be explained by two factors:

1) when the structure becomes disordered frustration of the antiferromagnetic bonds arises and results in fluctuations in the interaction of the nearest neighbors, as a result of which the "monolithic nature" of the antiferromagnetic state is destroyed;

2) the transition into the disordered state is accompanied by an increase in the average atomic displacement, resulting in the appearance of bonds characteristic for a ferromagnet.

The effect of local disorder on the exchange interaction was studied by Handrich in 1969.[106] He found that the exchange integral ΔJ_{ij} fluctuates around some average value

$$J_{ij} = \langle J_{ij} \rangle + \Delta J_{ij}, \tag{4.3}$$

where $\langle ... \rangle$ denotes averaging over the random bonds.

The exchange integral can be represented in the form of a Gaussian distribution

$$P(J_{ij}) = \frac{1}{\sqrt{2\pi}\Delta J} \exp\left[-\frac{(J_{ij} - J_0)^2}{2\Delta J^2} \right]. \tag{4.4}$$

According to the mean-field model the effect of the fluctuations in the exchange interaction is to lower the Curie temperature and smooth the curve of the magnetization versus the temperature. In this case the Curie temperature for the amorphous state T_c^a is expressed in the form

$$T_c^a = T_c^K \left(1 - \frac{Z}{Z\delta} \right), \tag{4.5}$$

where $\delta = \langle \Delta J^2 \rangle / J_0^2$, Z is the coordination number, and T_c^c is the Curie temperature of the crystalline state.

The temperature dependence of the magnetization is described by the equation

$$\frac{M(T)}{M(0)} = \frac{1}{2} B_s[(1 + \delta)x] + \frac{1}{2} B_s[(1 - \delta)x], \tag{4.6}$$

where B_s is the Brillouin function and $x = 3S(S+1)T_c/T$. The quantity δ ranges from 0 to 1 and is determined experimentally.

To calculate the chemical bonds in an amorphous metallic alloy Messmer[107] employed a tetrahedral cluster, consisting of Fe and Ni atoms and supplemented at the center with a boron atom. He found that the formation of metal-metalloid bound states qualitatively reduces the features of the d band and reduces the magnetic moment. The introduction of boron into a cluster results in broadening of the d band owing to hybridization with the $2p$ orbital of boron as well as in a decrease of the total energy of the states below that of the corresponding states for a cluster without a boron atom. In the process the stability of the amorphous state increases.

The essential feature of the model proposed by Corb *et al.*[108,109] is that for a given content of the metalloid M(M = B,Si,C,N) in alloys of the type $T_{1-x} - M_x$ the M atom is bound more to the T atom and is effective in suppressing magnetism. The degree of the p–d bonds is assumed to be proportional to the number of T atoms surrounding the atom M. The magnitude of the average magnetic moment per T atom in the amorphous alloy decreases owing to the increase in the number of coordination bonds between T and M. The average magnetic moment per T atom is

$$\mu_T = n \left(1 - \frac{Z_M^T N_M}{5N_T} \right), \tag{4.7}$$

where n is the number of valence electrons and N_T and N_M are the number of T and M atoms, respectively. The equation (4.7) presupposes that each T atom, located in a nearest neighbor environment of M atoms, forms with them a bond and, therefore, loses one-fifth of its magnetic moment because its fifth $3d$ electron orbital is bound by a nonmagnetic covalent bond.

Results demonstrating good agreement between the experimental data and the calculations based on the proposed model for an amorphous metallic alloy and crystalline solid solutions are presented in Fig. 6 for cobalt, which is a strong ferromagnet. The solid lines were calculated using Eq. (4.7) for $Z_B^{Co} = 6$ (upper curve) based on Co_3B, $Z_P^{Co} = 9$ (middle curve) based on the tetragonal structure Co_3P, and Z_P^{Co} changes from 12 (hexagonally close packed solid solution) with $N_M/N_{Co} = 0$ to $Z_P^{Co} = 9$ for $N_M/N_{Co} = 0.3$. It is believed that the bonds of the boron atoms decrease the magnetic moment of the six cobalt atoms, while the phosphorus atom, bound with nine cobalt atoms, gives an even sharper decrease of the magnetic moment. Corb *et al.*[108,109] believe that this model can also be extended to the metal-metal system. Based on everything said above we can conclude that the magnitude of the magnetic moment of a ferromagnetic element in a disordered state is determined by the short-range order and the interaction of electrons with the d shell.

Thus the models examined above make it possible to predict the magnetic moment and the Curie temperature of

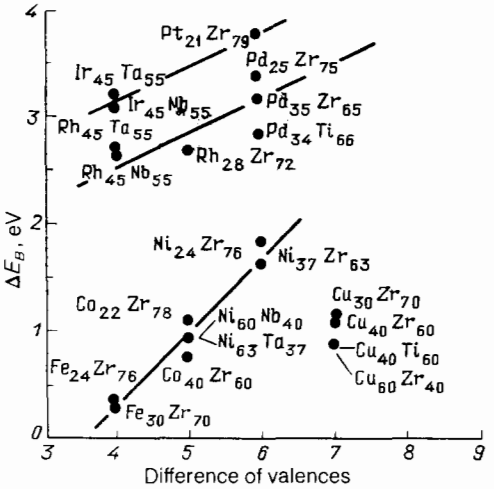

FIG. 6. The average magnetic moment per magnetic atom as a function of the ratio of the concentrations N_M/N_T of the nonmagnetic metalloid N_M to the transition element N_T. The solid line was calculated using Eq. (4.7) for the corresponding coordinate M.

the amorphous alloys $T_{1-x}M_x$. Significant difficulties are encountered when this question is examined for more complicated systems.

4.2. Spin glasses

Disorder, randomness, and frustration are problems that generate significant interest among physicists worldwide. The term "spin glass" was introduced by Coles in 1968 in order to distinguish magnetic amorphous materials with disordered arrangement of magnetic atoms in space from crystalline solid solutions in which the magnetic atoms usually occupy interstitial positions.

Spin glasses are magnetic systems in which the interaction of the magnetic moments is frustrated, and this frustration is caused by the "frozen" structural disorder. As in ferro- or antiferromagnets, in spin glasses there also exists a transition into the "frozen" state, characterized by a new type of order, in which the magnetic moments of the atoms are randomly oriented. The nature of this new type of order and its theoretical explanation have been under intense discussion in the last decade by many investigators (see Refs. 110–115 *et al.*).

Interest in spin glasses continues to increase because of the following circumstances.

1) Many condensed materials exhibit the properties of a spin glass. These include, first of all, systems with competing interaction between spins, i.e., crystalline alloys of metals of the type Fe_xAu_{1-x}, crystalline dielectrics of the type $Eu_xSr_{1-x}S$, and amorphous alloys $(Fe_{0.15}Ni_{0.85})_{75}P_{16}B_6Al_3$, $Tb_{90}Si_{10}$, and others. It was recently reported[116] that granular high-T_c superconductors exhibit the properties of a spin glass.

2) Attempts to sort out and understand the nature of the spin-glass state have led to the realization of the fact that the new concepts used to explain spin glasses can be used in other areas of science, for example, statistical mechanics and problems of optimization and computer technology.[115,117]

3) In spite of the intensive investigations, both experimental and theoretical, questions regarding the nature of the spin-glass state and especially the relaxation of such systems have not yet been completely explained.

The characteristic properties of spin glasses are determined from observations of the physical characteristics. Such observations include measurements of the magnetic susceptibility as a function of the temperature ($\chi(T)$), which permit determining, based on the presence of a maximum in the curve $\chi(T)$, the temperature of the transition into the spin-glass state T_f. The temperature T_f cannot be regarded as the phase-transformation point, since it depends strongly on the external magnetic field employed when measuring the frequency. The study of neutron-diffraction spectra shows that there are no magnetic Bragg peaks; this indicates that there is no long-range order in the arrangement of the magnetic moments at temperatures $T < T_f$. The transition into the spin-glass state does not affect the temperature dependence of the heat capacity $C(T)$. A wide peak is observed in the curve $C(T)$ at $T \sim 1.3T_f$. At the present time it is difficult to say anything definite about the reasons for the appearance of this anomaly in the heat capacity, but it is undoubtedly connected with the transition into the spin-glass state.

Measurements of the magnetization are a quite reliable indicator of the spin-glass state. Below T_f the magnetization depends on the history (the magnetization measured after cooling in a zero magnetic field differs from the magnetization obtained on cooling in a magnetic field). In all cases the residual magnetization decays very slowly with time. The use of other structurally sensitive methods for studying spin glasses raise hopes that other physical characteristics will also be sensitive to the transition into the spin-glass state. In particular, for example, in Ref. 117 it is reported that a peak was observed in the internal friction in the reentrant spin glass $Fe_{59}Ni_{21}Cr_{20}$ accompanying a transition into the frozen state.

The behavior of frozen magnetic moments in a spin glass does not resemble the ferromagnetic state, which is characterized by long-range order and spontaneous magnetization. In a spin glass there is no magnetization in zero magnetic field when the magnetic moments of the atoms are frozen in a random orientation and in the absence of long-range order. This concept presupposes that there is a significant difference between amorphous ferromagnets, paramagnets, and spin glasses. This difference is illustrated schematically in Fig. 7.

The main requirement for some kind of magnetic order in a solid is that there must exist magnetic moments that interact with one another. In systems with lanthanides, where the electrons are well localized, the magnetic moments can be coupled by means of isotropic Heisenberg exchange

$$H_{ij} = -2J_{ij}\mathbf{S}_i\mathbf{S}_j, \tag{4.8}$$

where J_{ij} is the exchange parameter between spins occupying the sites i and j. It is positive for ferromagnets and negative for antiferromagnets. In metallic dilute solid solutions the magnetic moments interact by the RKKY mechanism (Ruderman, Kittel, Kisuya, and Yoshida), the distinguishing feature of which is its long-range and oscillating nature. In the simplest case it is described in the form

$$J(R) = V_0 \cos(2k_F R + \varphi)(k_F R)^{-3}, \quad k_F R \gg 1, \tag{4.9}$$

where the effective parameter J between the spins separated

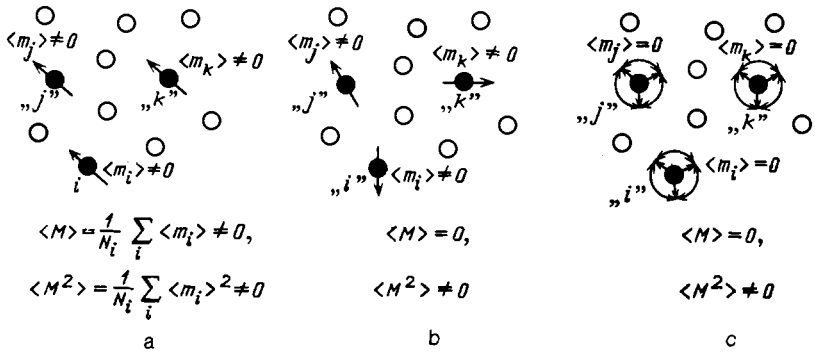

FIG. 7. Schematic representation of the differences between a ferromagnet below T_c (a), a spin glass below T_f (b), and a paramagnet (c). The open circles denote atoms of a nonmagnetic element, the dark circles with arrows denote the positions of atoms i, j, and k with magnetic moments responsible for the magnetization of the medium, N_i is the number of atoms with magnetic moments, $\langle m_i\rangle$, $\langle m_j\rangle$, and $\langle m_k\rangle$ are the thermally averaged magnetizations in the i, j, and k positions, and M is the average magnetization over all positions.

by a distance R decreases as R^{-3}. Here k_F is the wave vector of an electron at the Fermi level of the base metal; φ is a phase factor; V_0 is the coefficient proportional to J_{fs}, where J_{fs} is the exchange interaction between the localized f electrons and the conduction electrons.

The interaction between atoms separated by distances $R_0 \sim n^{-1/3}$ for $n/k_F^3 \ll 1$ is sign-alternating.[110] The sign-alternating interaction permits the atomic moments to interact with different probability with one another in both the ferromagnetic and antiferromagnetic manner. The presence of a random interaction of different sign results in competition between these two types of interactions. This fact is a determining feature in the physics of spin glasses.

Relaxational phenomena in spin glasses are of special interest. The first measurements of the relaxation time of the magnetization of spin glasses revealed a logarithmic time dependence.[110] Subsequent measurements revealed a significant deviation from a purely logarithmic dependence. Attempts to find the functional form of the relaxation continued and are continuing. The experimental data obtained with the help of different methods cover a time interval of up to 17 orders of magnitude: from 10^{-12} to 10^5 s. At temperatures below T_f the time dependence of the thermoremanent magnetization in a spin glass can be described by an exponential function of time[111]

$$M(t) \propto \exp\left(-\frac{t}{t_0}\right)^n, \tag{4.10}$$

where t_0 is the hold time at constant temperature and $0 < n < 1$. The decay of the magnetization depends on the hold time of the system. This indicates the existence of memory and the operation of the superposition principle. However this form should operate only for times less than the hold time t_0.

In accordance with the fractal-cluster model the rate of relaxation of the magnetization to the equilibrium state can be represented in the form[112]

$$\frac{\partial M}{\partial \ln t} \propto \left(\frac{t}{\tau_0}\right)^{-\beta/Z\nu} \exp\left[-\left(\frac{t}{\tau_{max}}\right)^{-\beta\delta/Z\nu}\right], \tag{4.11}$$

where β, δ, Z, and ν are the standard static and dynamic exponents, and

$$\tau_{max} = \tau_0\left(\frac{T}{T_f} - 1\right)^{-Z\nu}, \tag{4.12}$$

where τ_0 is the minimum relaxation time of the spin system (τ_0 can be regarded as the time necessary for one flipping of the spin magnetic moment and is equal to 10^{-13} s). Equation (4.12) reproduces the fundamental characteristics of relaxation effects in real spin-glass systems in a wide range of times and temperatures. Equation (4.11) leads to a slow change in the relaxation rate as $t \to \tau_{max}$, characterized by a weak power-law dependence (experiment and computer calculations give values for $\beta/Z\nu$ that fall within the limits 0.05–0.1). Using the usual values for the parameters determining the exponent Binder and Young[113] obtained for the spin glass $(Fe_{0.15}Ni_{0.85})_{75}B_{16}P_6Al_3$ ($\beta = 0.38$, $\delta = 10$, $Z = 8.2$ and $\tau_0 = 2\cdot 10^{-13}$ c satisfactory description of the time dependence of the experimentally observed relaxation rate near T_f. Thus Eq. (4.11) for the relaxation rate reproduces some fundamental characteristics of the relaxational effects in real spin-glass systems.

The search for analytic expressions for relaxation phenomena in spin glasses is nonetheless continuing. Theoretical and experimental methods, employing the excitation of elastic sign-alternating fields and making it possible to obtain information about structural relaxation processes in solids in the frequency range 10^{-5}–10^{12} Hz, deserve attention for studying relaxational processes in spin glasses.

Practical applications of spin glasses in microelectronics and other areas are significantly hampered by the absence of spin glasses with $T_f > 300$ K. In the last few years there have appeared experimental investigations in which efforts were made to prepare spin glasses with high values of T_f. Thus in Ref. 114 it is reported that the crystalline alloy $Tb_{62.5}Si_{37.5}$ has $T_f = 180$ K.

There have also appeared studies on the development of so-called cluster spin glasses. Thus in Ref. 115 heat treatment of the alloys $Cu_{3-x}Mn_xAl$ ($0.24 < x < 0.36$) was used to obtain a system which had inclusions of the ferromagnetic intermetallide Cu_2MnAl with average size ~ 4 nm. Measurements of the susceptibility showed that such a system is analogous to a spin glass, where accumulations of the intermetallide Cu_2MnAl play the role of spin magnetic moments. It is conjectured that if the average separation of the inclusions $l_c > d_c$ (d_c is the average size of the inclusions), then the magnetic moments of the inclusions interact by means of the RKKY indirect-exchange mechanism. Thus work on the development of new structures with the properties of a spin glass have only just begun and the development of this direction should lead to the realization of many still unknown theoretical and practical possibilities.

4.3. Magnetoelastic phenomena in amorphous alloys

For many years researchers have been interested, from both the theoretical and practical viewpoints, in magnetoe-

lastic damping, the ΔE effect, and other magnetoelastic phenomena.[118] In recent years interest in these phenomena has grown owing to the study of amorphous ferromagnets, where they are stronger than in crystals.[119,120] For example, in some amorphous alloys based on iron the ΔE effect can reach several hundreds of percent.[121] Magnetoelastic properties are determined by the effect of magnetic order on the elastic characteristics and are connected with the existence of the magnetostriction effect. Although in the theory of magnetism magnetostriction is a second-order effect, for amorphous metallic alloys, which are anomalously soft magnetically, magnetoelastic effects in many cases can be stronger than the first-order magnetic and elastic effects.

4.3.1. Magnetostriction

Magnetostriction is the most important parameter of a ferromagnet and is of interest both for the physics of the magnetic state and for practical applications. Knowledge about magnetostriction of amorphous magnetic alloys is necessary for solving fundamental problems of the magnetism of disordered structures and gives direct information about the character of the orbitals of the magnetic electrons.

When magnetic order appears spontaneously below the Curie temperature the volume and shape of the ferromagnetic material change. The application of external mechanical stresses in this case results in the appearance of, apart from purely elastic strain, and additional magnetostrictional strain, i.e., the total strain ε_{ij} is equal to

$$\varepsilon_{ij} = \varepsilon_{ij}^{s} + \varepsilon_{ij}^{m}, \tag{4.13}$$

where ε_{ij}^{s} are the components of the strain of the ferromagnet in a saturating magnetic field and ε_{ij}^{m} are the components of the magnetostrictional strain. The change in the components of the magnetostrictional strain tensor ε_{ij}^{m} in the ferromagnet phase depends on the direction and magnitude of the spontaneous magnetization M_s:[13]

$$\varepsilon_{ij}^{m} = \lambda_{ijkl} M_k M_l, \tag{4.14}$$

where λ_{ijkl} is the tensor of magnetostrictional elastic constants.

Just as in the case of the tensor of elastic constants, in this case there exist only two independent constants, describing the change in the volume and shape. If the magnetostrictional tensor is divided into purely volume $\varepsilon_{ij}^{m,v}$ and shear $\varepsilon_{ij}^{m,sh}$ parts, then[13]

$$\varepsilon_{ij}^{m} = \varepsilon_{ij}^{m,v} + \varepsilon_{ij}^{m,sh}, \tag{4.15}$$

where

$$\varepsilon_{ij}^{m,v} = \left(\frac{\omega_s}{3}\right)\delta_{ij}, \quad \omega_s = \sum_i \varepsilon_{ii} = \frac{\Delta V}{V}, \tag{4.16}$$

$$\varepsilon_{ij}^{m,sh} = -\frac{\lambda_s}{2}\delta_{ij} + \frac{3\lambda_s}{2}\frac{M_i M_j}{|M_s|^2}; \tag{4.17}$$

here ω_s is the relative change in volume $\Delta V/V$ owing to the spontaneous magnetization $M_s(T)$ and λ_s—the linear magnetostriction, i.e., the relative elongation $\Delta l/l$ of the sample in the direction of magnetization ($\theta = 0$), as compared with an imaginary sample with the same volume but with disordered magnetic moments, is given by

$$\frac{\Delta l}{l} = \frac{3}{2}\lambda_s\left(\cos^2\theta - \frac{1}{3}\right), \tag{4.18}$$

where θ is the angle between the direction of M_s and the direction in which $\Delta l/l$ is measured.

The spontaneous volume magnetostriction ω_s at a temperature T is described by the following expression:[12]

$$\omega_s(T) = \omega_s(0) - KCM^2(0,0)\left(\frac{T}{T_c}\right)^2, \tag{4.19}$$

where $\omega_s(0)$ is the spontaneous volume magnetostriction at 0 K; K is the compressibility; C is the coupling constant; $M(0,0)$ is the magnetization at 0 K and in zero magnetic field; and T_c is the Curie temperature. On the other hand the quantity $\omega_s(T)$ can be represented in the form

$$\omega_s(T) = 3\int_0^{T_c}(\alpha_p - \alpha_f)dT, \tag{4.20}$$

where α_p and α_f are the thermal linear expansion coefficient in the paramagnetic and ferromagnetic states, respectively. For amorphous alloys based on iron the total magnetoelastic increase in volume ω_s at 0 K is of the order of $1\cdot 10^{-2}$, which is comparable to the decrease in the volume observed when amorphous metallic alloys crystallize.

Experimental investigations of many amorphous alloys based on iron have shown[122] that in a wide temperature interval their magnetoelastic effects, leading to an increase in the volume as $|M_s|$ increases, i.e., $\omega_s > 0$, can compensate or even exceed the standard thermal expansion owing to anharmonicity of the vibrations of atoms. Thus, for example, in the interval 200–600 K the thermal expansion coefficient of the amorphous alloy $Fe_{33}B_{17}$ is zero, i.e., this alloy is a typical invar. Analyzing the experimental results for amorphous alloys Fe–B, Fe–P, Co–B, and others, Ishio and Takahashi[123] concluded that the zero thermal expansion coefficient is determined by the effective number of electrons n_{eff}, which is estimated based on the charge-transfer model as

$$n_{eff} = n_{TM} + \frac{1}{1+\sum_i x_i} x_i q_i, \tag{4.21}$$

where n_{TM} is the number of $3d + 4s$ electrons for each transition metal, x_i is the concentration of the ith metalloid, and q_i is the number of donor electrons of the ith metalloid. For B, Si, and P, q_i is equal to 1, 2, and 3, respectively. For the above-indicated alloys, irrespective of the type of metalloid, an alloy of the invar type corresponds to $n_{eff} = 8.2$. The same value of n_{eff} corresponds to magnetic instability in the amorphous state and a maximum magnetic moment for amorphous iron, obtained on a cooled substrate.

The change brought about in the shape of the sample (deformation at constant volume) by the presence of uniaxial anisotropy leads to the fact that the amorphous ferromagnetic has a linear magnetostriction λ_s. The experimental values of λ_s for most of the investigated amorphous alloys based on Fe–Co and Fe–Ni with a metalloid content of 20–25 at.%[124] fall in the range $(-10 \text{ to } 45)\cdot 10^{-6}$. Applications in electronic and electromagnetic devices require amorphous metallic alloys in the form of thin films and foils either with the strongest possible magnetostriction or with negligibly weak magnetostriction (close to zero). For example, different types of sensors and magnetoelastic transducers require materials with large value of λ_s. The highest values of λ_s, just as in the crystalline state, are found in amorphous metallic alloys based on rare-earth elements. Thus in amor-

phous alloys whose composition is close to that of $Tb_{50}Co_{50}$ gigantic magnetostriction ($\lambda_s \sim 2\cdot 10^{-4}$) was observed in significantly lower saturating fields (H = 3–4 kOe) than necessary for the crystalline analogs ($H > 100$ kOe).[125] It is conjectured[125] that magnetostriction in the amorphous alloys Tb–Co is determined primarily by the flipping of the magnetic moments of terbium, which in a zero magnetic field form a "fan," whose aperture angle is determined by the competition between the local magnetic anisotropy and the effective exchange-interaction field. In a field $H > 0$ the magnetic moments of the terbium ions are oriented along the field; this results in the appearance of gigantic magnetostrictional strains. Further investigations of the conditions required to produce amorphous alloys with gigantic values of λ_s and studies explaining these phenomena are undoubtedly necessary.

Devices and systems operating at high frequencies require amorphous metallic alloys with close to zero magnetostriction, since the magnetoelastic effects still degrade the magnetically soft properties. Amorphous metallic alloys based on cobalt and iron with zero magnetostriction were obtained already in the early studies of amorphous alloys. Later different types of amorphous alloys based on cobalt were obtained by sputtering. These alloys contained the nonmagnetic elements Zr, Hf, Ti, Nb, Ta, W, and Mo as the glass-forming elements. Alloys with both positive and negative λ_s were obtained. They also included the alloys $Co_{85}Nb_{7.5}Ti_{7.5}$ and $Co_{86}Nb_7Zr_{3.5}Mo_{3.5}Cr_{1.5}$ with zero magnetostriction.[126,127] The magnetostrictional properties of the amorphous alloys $(Co_{1-x}Fe_x)_{85}Nb_{15}$ have been the most studied.[128] The curves of λ_s as a function of the concentration x are described by the parabolic equation

$$\lambda_s \cdot 10^6 = \alpha x^2 + 2\beta x(1-x) + \gamma(1-x)^2, \qquad (4.22)$$

where α, β, and γ are constants determined from the data on λ_s. The equation (4.22) is equivalent to the theoretical dependence of λ_s on x in alloys of the binary system $A_{1-x}B_x$, based on the dipole-type magnetic interaction of atomic pairs.

Studying the reasons for the appearance of zero magnetostriction in amorphous magnetic alloys of the type $(Fe_xCo_{1-x})_{1-y}(Si_{0.4}B_{0.6})_y$ and using the single- and two-ion model to explain magnetostriction Balasubramanian *et al.*[129] and Gonzalez and du Tremolet de Lacheisserie[130] came close to solving the problem of determining the basic characteristics of the ferromagnetic state.

4.3.2. The ΔE effect in amorphous alloys

Magnetoelastic coupling changes the elastic modulus, which can be regarded as a superposition of separate contributions:[131]

$$E = E_p - E_m, \qquad (4.23)$$

where E_p is the "paramagnetic" elastic modulus, obtained by extrapolating the dependence $E(T)$ from the paramagnetic region, and E_m is the "magnetic" contribution of the elastic modulus, which consists of three components:

$$E_m = \Delta E_a + \Delta E_\omega + \Delta E_\lambda; \qquad (4.24)$$

here ΔE_a and ΔE_ω are determined by the change brought about by magnetic ordering in the binding forces and the

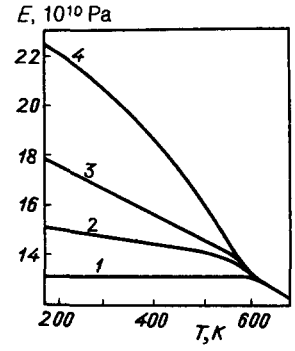

FIG. 8. The temperature dependence of Young's modulus in the amorphous alloy $Fe_{82}B_{12}$ measured in a magnetic field of strength $H = 0$ (*1*), 0.96 (*2*), 1.36 (*3*), and 112 (*4*) kA/m.

change produced by the magnetic field in the volume contribution, respectively, and ΔE_λ is characterized by the change brought about in the domain structure by external stresses.

Investigations of the ΔE effect in amorphous ferromagnets have shown that in amorphous metallic alloys based on the transition metals iron, cobalt, and nickel the main contribution to the change in the elastic modulus is connected with the change brought about in the domain structure by external mechanical stresses. Figure 8 shows the temperature dependence of Young's modulus in the amorphous metallic alloy $Fe_{82}B_{18}$ after isothermal annealing at $T = 573$ K during a period of two hours.[132] In the absence of a magnetic field E is virtually independent of the temperature, and thus below the Curie temperature this alloy is a typical Elinvar material. In a field $H = 112$ kA/m at room temperature E changes approximately by 70% (curve 4), and this increase is connected with both components ΔE_a and ΔE_λ (the component $\Delta E_\omega \approx 0$). However it is difficult to make an accurate determination of the components ΔE_a and ΔE_ω, determined by the difference between E_s (measured in a saturation magnetic field) and the elastic modulus obtained by extrapolation from the paramagnetic state, since the Curie temperature of amorphous metallic alloys is close to T_x. Therefore the extrapolated curves are poorly determined. For this reason, in studying the ΔE effect in amorphous metallic alloys the component of the elastic modulus ΔE_λ whose appearance is closely related with existence of ε^m, is usually studied. In magnetostrictional alloys in the presence of an external magnetic stress σ_{ij} the magnetoelastic energy[133] can be written in the form

$$W_\lambda = -\sum_{i,j} \sigma_{ij}\varepsilon_{ij}^m, \qquad (4.25)$$

which under the action of uniaxial tensile stress σ assumes the form

$$W_\lambda = -\frac{3}{2}\lambda_s \sigma \cos^2\theta, \qquad (4.26)$$

where λ_s is the linear saturation magnetostriction and θ is the angle between the spontaneous magnetization vector and the direction of σ. From the condition that the energy should be minimum when a ferromagnet with positive magnetostriction is stretched, according to Eq. (4.26), it follows that the angle $\theta \to 0$, i.e., the spontaneous-magnetization vector is aligned parallel to the stretching force, while for a ferromagnet with negative magnetostriction $\theta \to 90°$, i.e., the magneti-

zation is perpendicular to the stretching force. As a result of the rotation of the spontaneous-magnetization vectors, caused by the tensile stress, in a ferromagnet with either sign of λ_s an excess relative stretching is created and the modulus of elasticity decreases. The magnitude of the ΔE effect shows the relative contribution of the magnetic strain ε^m to the total elastic strain ε, i.e.,[94]

$$\frac{\Delta E}{E} = \frac{E_s - E_0}{E_0} = \frac{\varepsilon^m}{\varepsilon}, \tag{4.27}$$

where E_s is the modulus of elasticity measured in a saturating magnetic field and E_0 is the modulus of elasticity measured in the absence of a magnetic field. The numerical value of the ΔE effect depends on the magnetostriction, the magnitude of the internal stresses, and the orientation of the magnetization vectors of the domains relative to the external uniaxial stress:[13]

$$\frac{\Delta E}{E} = \frac{E_s - E_H}{E_H} = \frac{3E_s|\lambda_s|}{\sigma_i/\cos^2\theta \cdot \sin^2\theta}, \tag{4.28}$$

where E_H is the modulus of elasticity measured in a magnetic field of strength H and σ_i is the internal stress. The dependence of the ΔE effect on the strength of the external magnetic field for the amorphous ferromagnet $Fe_{74}Co_{10}B_{16}$ with different domain structure and different orientation of the external mechanical stress[134,135] is shown in Fig. 9, where the ΔE effect was calculated according to the formula $\Delta E/E = (E_H - H_0)/E_0$. In alloys with a complicated domain structure, which were obtained by quenching from the liquid state (QLS), the ΔE effect assumes small negative values in weak magnetic fields ($H < 400$ A/m), after which it increases monotonically and saturates (curve *1*). This dependence of $\Delta E/E = F(H)$ is characteristic for many crystalline ferromagnets. In amorphous alloys with a striped domain structure, which are obtained by the method of ion-plasma sputtering (IPS), when the magnetization vector lies in the plane of the film, the magnitude of the ΔE effect depends on the orientation of the applied stress relative to the axis of easy magnetization. When the axis of easy magnetization is parallel to the applied stress the ΔE effect is not observed (curve *2*), and when the axis of easy magnetization is perpendicular to the applied stress a negative ΔE effect occurs for all values of the strength of the external magnetic field (curve *3*). Such an unusual dependence is characteristic only for amorphous magnetic alloys and is described well by the expression (4.20). In the model of coherent rotation of magnetic moments,[136] calculated for this case, it is shown that for strengths of the external magnetic field $H < 2K_u/M$

$$\frac{\Delta E}{E} = 9\lambda_s^2 E_s M_s^2 H^2 (2K_u)^{-3}, \tag{4.29}$$

where K_u is the magnetic anisotropy energy and M_s is the saturation magnetization, the ΔE effect must be proportional to the squared magnetostriction, but this model has not been checked experimentally.

The difference in the domain structure of alloys with identical composition gives rise to different mechanisms for the change in magnetization of the material. In a material prepared by the method of quenching from the liquid state the magnetization changes by means of the displacement of the domain walls as well as a result of the rotation of the magnetization vector. However in alloys obtained by the method of ion plasma sputtering there are no 90° walls and the 180° walls are oriented perpendicular to the applied field, and for this reason the magnetization along the longitudinal axis of the sample is produced by the rotation of the magnetization vectors. This difference is also reflected in the dependence of the magnitude of the ΔE effect on the frequency of the mechanical oscillations, as shown in Fig. 10 in the coordinates $|\Delta E/E| = F(f^{-1/2})$.[135] Thus the absence of a frequency dependence of the ΔE effect for alloys prepared by the method of quenching from the liquid state, right up to $f \sim 400$ kHz, indicates that the domain walls affect most the change produced in the magnetization of the material by mechanical stresses. Increasing further the frequency of mechanical oscillations results in the fact that the oscillating displacements of the domain walls cannot follow the change in the sign-alternating stresses and the ΔE effect diminishes. In an amorphous alloy prepared by the method of ion-plasma sputtering the dependence of the ΔE effect on the frequency of the mechanical oscillations arises primarily because of eddy currents, which, owing to the skin effect, diminish the magnitude of the ΔE effect in proportion to $f^{1/2}$. The fact that the skin effect affects the magnitude of the ΔE effect is indicated by the data in Ref. 137, which were obtained for the amorphous alloys $Fe_{45}Co_{45}Zr_{10}$ of different thicknesses (Fig. 11). Thus, at the frequency $f = 1$ mHz

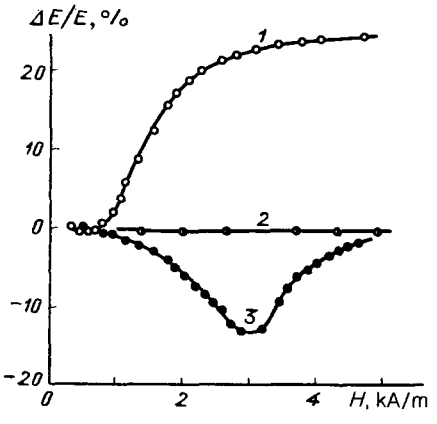

FIG. 9. The ΔE-effect in the amorphous alloy $Fe_{74}Co_{10}B_{16}$ prepared by the method of quenching from the liquid state (*1*), the method of ion-plasma sputtering with magnetization parallel (*2*) and perpendicular (*3*) to the easy axis of magnetization.

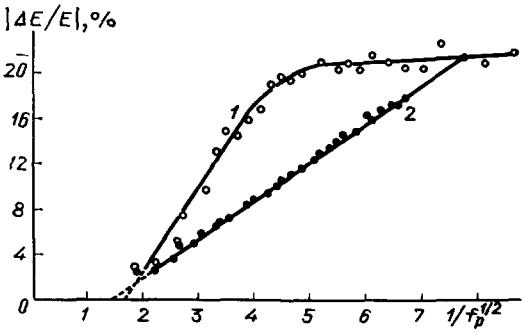

FIG. 10. The frequency dependence of the ΔE-effect in the amorphous alloy $Fe_{74}Co_{10}B_{16}$ prepared by the method of quenching from the liquid state (*1*) and ion-plasma sputtering (*2*).

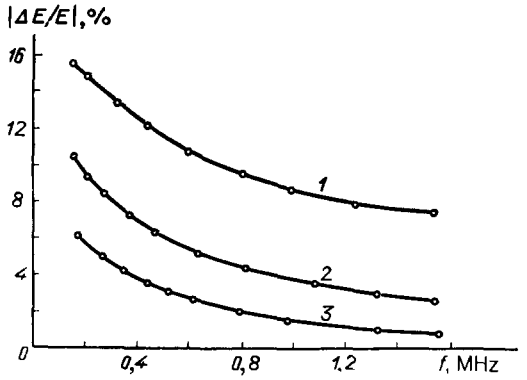

FIG. 11. The frequency dependence of the ΔE-effect in the amorphous alloy $Fe_{45}Co_{45}Zr_{10}$ for samples with different thicknesses (in μm): 10 (1), 40 (2), and 120 (3).

with a thickness $h = 120\,\mu$m $\Delta E/E \sim 2\%$ (curve 3), while for $h = 10\,\mu$m the ΔE effect increases to 9% (curve 1).

The values of the ΔE effect have now been determined for many metal-metalloid and transition metal–rare-earth-metal systems. Table III gives values of the maximum ΔE effect obtained as the difference between E_s and the minimum value E_H in the kilohertz frequency range for different amorphous metallic alloys. Analysis of the table shows that the high values of the ΔE effect were obtained after heat and thermomagnetic treatments. In the case of the heat treatment, the internal stresses decrease as a result of structural relaxation; this reduces the magnetoelastic anisotropy and increases the magnetoelastic properties. Figure 12 shows the ΔE effect in the amorphous alloy $Fe_{81}B_{15}Si_4$ as a function of the temperature and the duration of isothermal annealing.[142] At the first stage of annealing the magnitude of the ΔE effect increases; this is connected with relaxation and the decrease in the internal stresses preventing the motion of domain walls. However for some values of the temperature and duration of annealing the magnitude of the ΔE effect decreases appreciably. This is especially noticeable if the isothermal holding is conducted below the Curie temperature; this stabilizes the domain walls. Better results can be obtained if the crystallization temperature of the amorphous metallic alloy is higher than the Curie temperature. In this case annealing in the temperature interval between T_c and T_x followed by fast cooling results in an increase of the ΔE effect. Another method that makes it possible to decrease the stability of the domain walls is annealing in a magnetic field oriented perpendicular to the longitudinal axis of the sample. In this case, apart from the decrease in the internal stresses, there forms a domain structure that permits realizing maximum values of magnetostriction along the longitudinal axis of the sample and makes possible "gigantic values of the ΔE effect.

Thus investigations of the ΔE effect in amorphous metallic alloys have led to the development of a significant number of ferromagnetic amorphous metallic alloys with high magnetoelastic properties in the kilohertz frequency range. Practical applications (for example, in controllable signal-delay lines) require materials with a high ΔE effect in the megahertz frequency range. Further work in this direction should lead to the development of materials based on amorphous metallic alloys that will make it possible to realize a gigantic ΔE effect at frequencies of 1–50 MHz.

4.3.3. Magnetomechanical damping

In magnetostrictional amorphous metallic alloys, aside from damping of elastic oscillations for nonferromagnetic reasons, there arise additional energy losses connected with the existence of magnetoelastic coupling in these materials. Internal friction in this case (with the exception of damping of a nonmagnetic nature) can be represented in the form of three terms:

$$Q^{-1} = Q^{-1}_{max} + Q^{-1}_{min} + Q^{-1}_r, \qquad (4.30)$$

where Q^{-1}_{max}, Q^{-1}_{min} and Q^{-1}_r are the damping of elastic oscillations that is connected with the existence of macro- and microeddy currents and hysteresis, respectively. The magnitude of the damping and the dominant component of the magnetoelastic internal friction depend on the type of domain structure of the material and the conditions of measurement (the frequency of mechanical oscillations and the orientation of the applied mechanical stress relative to the magnetization vector of the domains). In amorphous metallic alloys prepared by the method of quenching from the liquid state, at frequencies $f < 10^5$ Hz the main contribution to the damping of elastic oscillations is connected with magnetomechanical hysteresis—irreversible motion of 90-degree domain walls. This is indicated by the strong amplitude dependence of the internal friction[119,143] and the fact that the magnetoelastic properties are constant in this range of frequencies.[144] The high damping in this case is realized in the absence of strong stoppers, which interfere with the motion of the domain walls. In crystalline ferromagnets the fac-

TABLE III. The maximum changes in the modulus of elasticity in some amorphous metallic alloys at room temperature.

Alloy	$\Delta E/E$	Annealing conditions			References
		Time, min	Temperature, K	Field	
$Fe_{82}B_{18}$	0,7	120	643	—	[132]
$Fe_{75}P_{15}C_{10}$	0,8	30	573	$H_\perp$	[138]
$Fe_{78}B_{12}Si_{10}$	1,75	5	646	—	[139]
$Fe_{71}Co_9B_{20}$	2,2	15	657	—	[139]
$Fe_{80}B_{15}Si_5$	4,5	2	623	$H_\perp$	[140]
$Fe_{81}B_{13,5}Si_{3,5}C_2$	2	—	—	$H_\perp$	[141]
$Fe_{81}B_{15}Si_3C_1$	2,36	15	663	$H_\perp$	[121]
$Fe_{81}B_{15}Si_4$	2,77	2	663	$H_\perp$	[142]

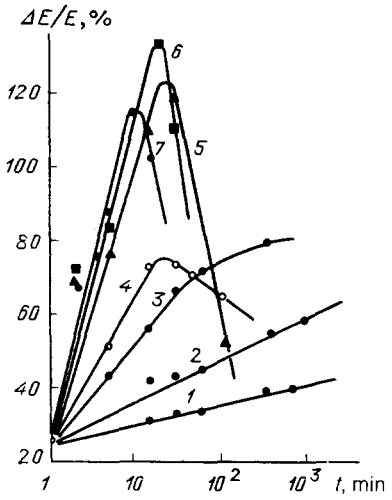

FIG. 12. The ΔE-effect in the amorphous alloy $Fe_{81}B_{15}Si_4$ at room temperature as a function of the isothermal annealing time for annealing temperatures $T = 473$ (*1*), 523 (*2*), 573 (*3*), 623 (*4*), 648 (*5*), 673 (*6*), and 698 (*7*) K.

tors resisting the motion of domain walls are crystallographic anisotropy and defects in the crystal lattice (grain boundaries, dislocations, etc.). Amorphous metallic alloys do not have the crystallographic anisotropy and many structural defects inherent in crystalline alloys. The main stoppers, preventing the motion of domain walls, in them are defects of the amorphous structure which give rise to internal stresses. The magnitude of the internal stresses can be estimated from measurements of the amplitude dependence of the internal friction (Fig. 13). In Ref. 145, under the assumption that the distribution function of the internal stresses is Maxwellian, expressions were derived that relate the parameters of the magnetomechanical damping with the average internal stresses σ_i, i.e.,

$$Q^{-1} \sim \frac{\sigma \lambda_s E}{\sigma_i^2} \quad \text{for} \quad \sigma \ll \sigma_i, \tag{4.31}$$

where σ is the amplitude of the internal stresses. The maximum magnitude of the damping

$$\Delta Q^{-1} \sim \frac{\lambda_s E}{\sigma_i} \tag{4.32}$$

is observed when

$$\sigma_m = 0{,}7256\sigma_i; \tag{4.33}$$

here ΔQ^{-1} is the height of the maximum in the amplitude dependence of the internal friction; σ_m is the amplitude of the stresses that corresponds to the maximum in the curve $Q^{-1}(\varepsilon)$. In Ref. 119 the magnitude of the internal stresses was estimated for the amorphous alloy $Fe_{40}Ni_{40}P_{14}B_6$ with the help of Eq. (4.33) and the data in Fig. 13. The estimates made of the magnitude of the internal stresses showed that heat treatment of the alloy $Fe_{40}Ni_{40}P_{14}B_6$ can reduce the stresses from $1.5 \cdot 10^7$ to $2 \cdot 10^6$ Pa, i.e., by almost an order of magnitude. This result indicates that the concentration of defects of the amorphous structure, which prevent the displacement of domain walls under the action of mechanical stresses and which increase the internal friction by more than an order of magnitude, decreases.

At higher frequencies the contribution of the eddy currents to the total internal friction increases. Figure 14 shows the frequency dependence of the internal friction of the amorphous alloy $Fe_{45}Co_{45}Zr_{10}$ with a striped domain structure,[137] whose easy-magnetization axis is oriented perpendicular to the longitudinal axis of the sample, along which the elastic waves were excited. Measurements performed in a magnetic field H corresponding to maximum damping showed (Fig. 14) that the height and position of the maximum of internal friction depend strongly on the thickness of the material. This is a characteristic feature of the losses

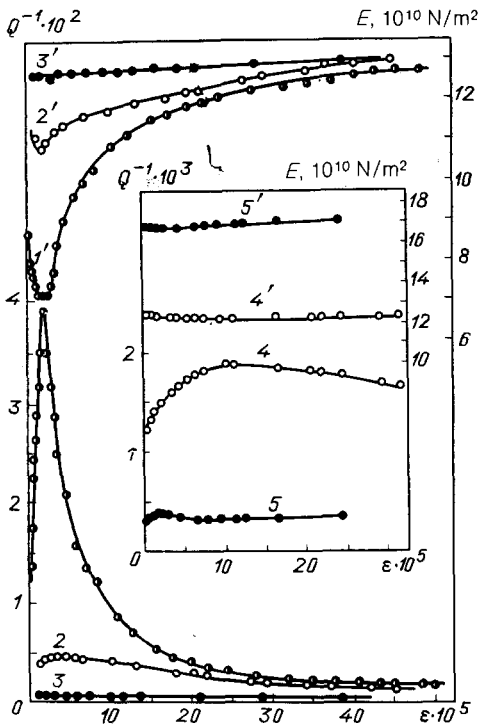

FIG. 13. The amplitude dependences of the internal friction and the modulus of elasticity of the alloy $Fe_{40}Ni_{40}P_{14}B_6$ in the starting state (curves *4* and *4′*), the crystalline state (curves *5* and *5′*), and the states (*1*, *1′*) after thermomagnetic treatment (curves *1*, *1′–3*, *3′*); the measurements were performed in the field $H = 0$ (*1*), 1 (*2*, *2′*), and 10 (*3*, *3′*) kA/m.

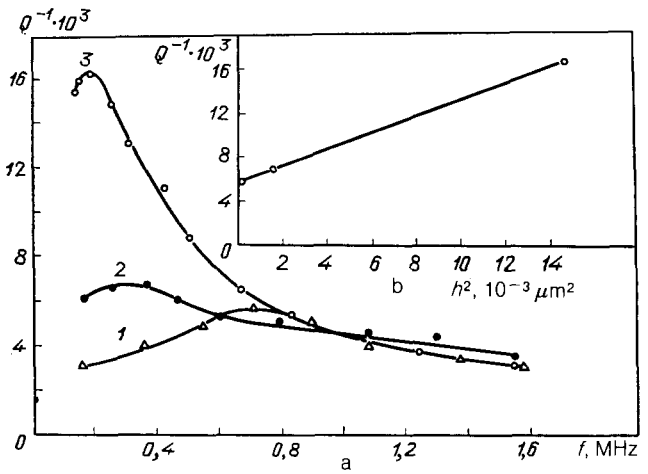

FIG. 14. The frequency dependence of the internal friction in the amorphous alloy $Fe_{45}Co_{45}Zr_{10}$ for thicknesses of 10 (*1*), 40 (*2*), and 120 (*3*) μm.

associated with macroeddy currents[97]

$$Q^{-1} \sim \frac{\omega h^2}{D_m}, \tag{4.34}$$

where ω is the angular frequency, h is the thickness of the sample, and D_m is the diffusion coefficient. In the limiting case of high frequencies the eddy-current damping is determined by the frequency dependence of the depth of the skin layer and is proportional to $f^{-1/2}$.

Maximum losses associated with microeddy currents are also expected in the frequency range 10^5–10^6 Hz.[146] However, because their contribution to the total magnetoelastic damping in the pure form in amorphous metallic alloys is small they have not been observed.

Thus from the physical standpoint the same damping mechanisms are realized in ferromagnetic amorphous metallic alloys as in crystalline ferromagnets. However because of the lower anisotropy and the absence of structural defects characteristic of crystals (grain boundaries, twins, etc.) the damping of mechanical oscillations is stronger in amorphous metallic alloys. This makes amorphous metallic alloys promising materials with a high damping capability which are suitable for applications in the building of instruments.

5. CONCLUSIONS. POSSIBLE APPLICATIONS OF AMORPHOUS METALLIC ALLOYS

The technology for preparing amorphous metallic alloys by quenching from the liquid state has made it possible for physicists and materials scientists to discover a number of new physical phenomena and properties and to employ them in many applications. Unfortunately, some practical applications of amorphous metallic alloys, prepared by the method of quenching from the liquid state, have not completely lived up to their promise, for example, for the development of high-power transformers or heavy-duty constructional parts. However there exist very many other possibilities for using amorphous metallic alloys both in the development of new technology and in studying physical phenomena, if other methods of preparation are employed: ion-plasma method, laser-induced vitrification ion implantation, etc.

1. As is well known, *the diffusion of atoms is accelerated significantly in the presence of interphase boundaries and grain boundaries.* A lower rate of diffusion is characteristic for single-crystalline layers, in which diffusion along lattice sites predominates. Experimental data for a large number of materials show that diffusion along lattice sites is most noticeable and occurs quite rapidly at temperatures above $0.7T_m$ (T_m is the melting point), while diffusion along grain boundaries occurs at temperatures above $0.5T_m$. From here it can be concluded that in the technology of production of microelectronic devices single-crystalline layers are most desirable, but for the existing level of the technology this is difficult to achieve. For this reason, in the last few years the question of the application of amorphous metallic alloys prepared by the method of ion-plasma sputtering as an alternative to single-crystalline layers has started to be discussed. In relaxed amorphous metallic alloys there are no grain boundaries or dislocations characteristic of the crystalline state, the structure is more homogeneous, and diffusion along the vacancies is slower, since vacancy-like defects often are smaller than vacancies in the crystal lattice. Thus amorphous metallic alloys are potential candidates for use as barrier layers blocking diffusion. Of course, it is necessary to choose alloys whose crystallization temperature is higher than the technological formation temperature of the integrated device. Another characteristic property of amorphous metallic alloys is the relative technological simplicity of producing any kind of geometric configurations on large areas. This feature, together with the capability of obtaining in a single technological cycle semiconductor and insulator layers, makes amorphous metallic alloys promising for applications in microelectronics.

In 1985 a patent entitled "Semiconductor devices employing amorphous metallic layers as contacts" was published.[147] The amorphous alloys Ni–Nb, Ni–Mo, Mo–Si, W–Si are recommended as a new class of materials for metalization, that can be used as the first metal coating, and diffusion-blocking barriers as well as corrosion-resistant coatings.

The main drawback of the proposed amorphous metallic alloys is their relatively low crystallization temperature (850–1000 K), which makes it impossible to use them in a technological process with heating above 1000 K. In the last few years[148,149] new amorphous layers, which remain amorphous even with heating up to 1300–1400 K, have been developed. These are alloys of rhenium with tantalum, titanium, and niobium. Thus it is entirely possible to increase significantly the thermal stability of metal-semiconductor contacts with the use of amorphous metallic alloys. There is

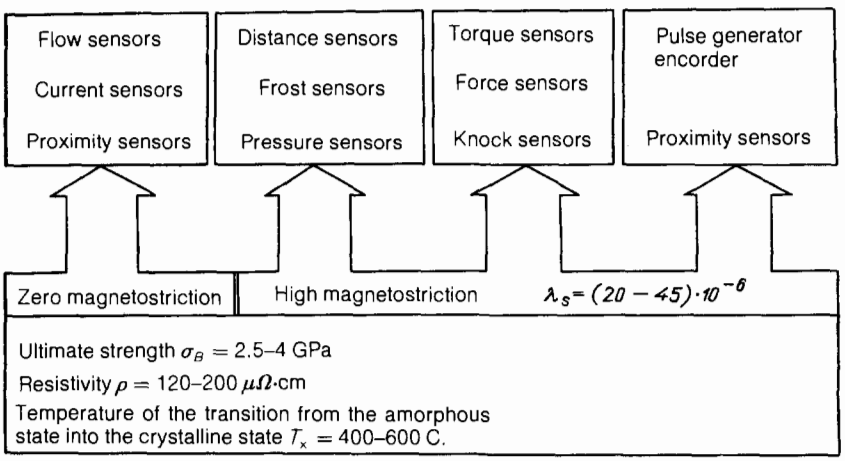

FIG. 15. Diagram of the possible applications of amorphous alloys as sensors and transducers.

no doubt that such amorphous alloys are promising as anti-diffusion barriers.

2. *Amorphous metallic alloys as a material for magnetic heads and different types of transducers and sensors.* The technology for preparing amorphous metallic alloys by the method of ion-plasma sputtering, which makes it possible to obtain layers $1-10^4$ μm thick, has already been developed in the laboratory. Thin layers often have unique physical properties, and this makes it possible to solve very complicated problems in instrument building. It is well known that ferromagnetic materials are employed for recording and storing information. To increase the information density materials in which the size of a single carrier does not exceed 1 μm are under development. Such carriers have a high coercive force (1500–2000 Oe). To work with such carriers it is necessary to have magnetic heads in which amorphous metallic alloys must be the main working element. The traditionally employed ferrite cannot be used, since the saturation induction in magnetic heads made of this material does not exceed $0.45-0.50T_d$, and the brittleness and crystallinity make it impossible to obtain a head with a working part less than 10 μm in size. Sputtering makes it possible to obtain from an amorphous metallic alloy a magnetic head with induction $B = 1-1.4T_d$, dimensions as small as desired, for example, capable of remagnetizing a particle 0.01 μm in size. The core of the head has minimum anisotropy and relative permeability $\mu = 1000-2000$ at frequencies of 5–20 MHz with saturation magnetostriction close to zero.

Amorphous layers can also find wide application in the development of highly sensitive transducers, sensing devices, and different converters. Figure 15, which was taken from Ref. 150, presents some properties of amorphous metallic alloys and the possible areas of application. As one can see from this diagram, amorphous metallic alloys can be used in two areas: different types of magnetic-field meters (magnetometers), magnetic heads, where alloys with zero magnetostriction must be employed, and sensors (sensors of voltages, strain, velocity, rotation, etc.), where alloys with high magnetostriction are employed. Amorphous metallic alloys are most effectively used by Japanese companies. Thus the Matsushita Company employs in the production of a commercial computer 361 different types of sensors made from ferromagnetic amorphous metallic alloys.

In conclusion we note that amorphous alloys with high values of the ΔE effect at frequencies above 1 MHz are promising. Thus, for example, for the amorphous alloy $Fe_{74}Co_{10}B_{16}$, prepared in the form of a film 5 μm thick, the ΔE-effect reaches values of 20% at frequencies of 1–1.5 MHz.[151] Such an alloy with amorphous structure can be employed to fabricate magnetic-field-controlled delay lines operating at megahertz frequencies.

[1] J. Ziman, *Models of Disorder: The Theoretical Physics of Homogeneously Disordered Systems*, Cambridge University Press, N.Y., 1979 [Russ. transl., Mir, M., 1982].
[2] A. Shalnikov, Nature **142**, 74 (1938).
[3] A. Shalnikov, Zh. Eksp. Teor. Fiz. **10**, 630 (1940).
[4] I. V. Salli, *Physical Foundation of the Formation of the Structure of Alloys* [in Russian], Metallurgizdat, M. 1963.
[5] P. Duwez, R. H. Willens, and W. Klemen, J. Appl. Phys. **31**, 1136 (1960).
[6] A. F. Skrishevskiĭ, *Structural Analysis of Liquids and Amorphous Bodies* [in Russian], Vysshaya shkola, Moscow (1980).
[7] C. Wagner and H. Ruppersberg, Atom. Ener. Rev., Suppl. **1**, 101 (1981).
[8] A. Sadoc and J. C. Lasjannias, J. Phys. F **15**, 1021 (1985).
[9] V. V. Nemoshkalenko, A. V. Romanova, A. G. Il'inskiĭ *et al.*, *Amorphous Metallic Alloys* [in Russian], Naukova dumka, Kiev (1987).
[10] H. Guntherodt and H. Beck [Eds.], *Glassy Metals I: Ionic Structure, Electronic Transport, and Crystallization*, Springer-Verlag, N.Y., 1981 [Russ. transl., Mir, M., 1983].
[11] K. Sudzuki, H. Fudzimori, and K. Hasimoto in *Amorphous Metals* [Russ. transl.], edited by Ts. Masumoto, Metallurgiya, M., 1987.
[12] F. E. Lyuborskiĭ [Ed.], *Amorphous Metallic Alloys* [in Russian], Metallurgiya, Moscow (1987).
[13] H. Guntherodt and H. Beck [Eds.], *Glassy Metals II: Atomic Structure and Dynamics, Electronic Structure, and Magnetic Properties*, Springer-Verlag, N. Y., 1983 [Russ. transl., Mir, M., 1986].
[14] D. S. Belashchenko, *Structure of Liquid and Amorphous Metals* [in Russian], Metallurgiya, M., 1985.
[15] V. A. Polukhin and N. A. Vatolin, *Modeling of Amorphous Metals* [in Russian], Nauka, M. 1985.
[16] P. H. Gaskell, Nature **276**, No. 5687, 484 (1978).
[17] P. H. Gaskell, J. Non-Cryst. Solids **32**, 207 (1979).
[18] V. A. Likhachev and V. E. Shudegov, *Structure and Properties of Amorphous Alloys* [in Russian], Ustinov (1985), p.14.
[19] V. A. Likhachev and A. I. Mikhaĭlin, Fiz. Khim. Stekla **14**, 161 (1988).
[20] H. Koizumi and T. Ninomiya, J. Phys. Soc. Jpn. **49**, 1022 (1980).
[21] C. L. Briant and J. J. Burton, Phys. Status Solidi B **85**, 393 (1978).
[22] R. Wang, Nature **278**, No. 5706, 700 (1979).
[23] A. Felt, *Amorphous and Glassy Inorganic Solids* [Russ. transl., Mir, M., 1986].
[24] P. J. Steinhardt, Am. Sci. **74**, 586 (1986).
[25] D. Gratia, La Recherche Nr. **178**, 788–798 (June 1986).
[26] J. D. Bernal, Nature **185**, 68 (1960).
[27] D. E. Polk, Acta Metall. **20**, 485 (1972).
[28] G. S. Cargill III, Atom. Energy Rev., Suppl. **1**, 63 (1981).
[29] D. Weaire, "*Excitons in disordered systems*," Proceedings of the NATO Adv. Study Inst. Eastern, Aug. 23–Sept. 4, 1981, Lausky, Michigan (1982), p. 579.
[30] J. L. Finney, Nature **266**, 309 (1977).
[31] T. Ninomiya, *Structure of Non-Crystalline Materials*, N.Y., 1982, p. 558.
[32] W. H. Zachariasen, J. Am. Chem. Soc. **54**, 3841 (1932).
[33] V. A. Polukhin and N. A. Vatolin, *Physics of Amorphous Alloys* [in Russian], Izhevsk, 1984, p. 26.
[34] Yu. I. Maslennikov, *Physics of Disordered Systems* [in Russian], Ustinov, 1986, No. 8, p. 42.
[35] Yu. I. Maslennikov, Rasplavy **1**, No. 4, 75 (1987).
[36] Yu. A. Kunitskiĭ, V. N. Korzhik, and Yu. S. Borisov, *Noncrystalline Metallic Materials and Coatings in Technology* [in Russian], Tekhnika, Kiev, 1988.
[37] I. V. Zolotukhin, *Physical Properties of Amorphous Metallic Materials* [in Russian], Metallurgiya, M., 1986.
[38] Yu. R. Zakis, *Physics and Chemistry of Glass-Forming Systems* [in Russian], Riga, 1980, p. 3.
[39] Yu. R. Zakis, Glass '89. Survey Paper 15th International Congress on Glass, Leningrad, 1989, p. 234.
[40] F. Spaepen, *Physics of Defects*, Amsterdam, 1981, p. 133.
[41] D. K. Belashchenko, Fiz. Met. Metalloved. **53**, 1076 (1982) [Phys. Met. Metallogr. (USSR) **53**(6), 28 (1982)].
[42] A. M. Glezer, B. V. Molotilov, and O. L. Utevskaya, Dokl. Akad. Nauk SSSR **263**, 84 (1982) [Sov. Phys. Dokl. **27**, 250 (1982)].
[43] T. Egami, K. Maeda, and V. Vitek, Philos. Mag. A **41**, 883 (1980).
[44] D. Srolovitz, K. Maeda, V. Vitek, and T. Egami, *ibid.* **44**, 847 (1981).
[45] T. Egami and V. Vitek, J. Non-Cryst. Solids **61–62**, 499 (1984).
[46] Y. Adda, G. Brebec, R. Gupta, and Y. Limoge, Mater. Sci. Forum **15–18**, 349 (1987).
[47] H. Kronmuller and W. Fernengel, Phys. Status Solidi A **64**, 593 (1981).
[48] D. R. Nelson, Phys. Rev. B **28**, 5515 (1983).
[49] J. F. Sadoc, J. Phys. Lett. **56**, 707 (1983).
[50] J. F. Sadoc and R. Mosseri, J. Phys. (Paris) **45**, 1025 (1984).
[51] G. E. Abrosimova, A. S. Aronin, and L. V. Voropaeva, Metallofiz. **11**, 102 (1989).
[52] L. A. Zhukova and S. I. Popel', Izv. Akad. Nauk SSSR, Metally, No. 2, 173 (1984).
[53] O. V. Mazurin, *Glass Formation and Stability of Inorganic Glasses* [in Russian], Nauka, Leningrad, 1978.
[54] M. Gibbs and C. Hygate, J. Phys. F **16**, 809 (1986).
[55] Y. Waseda and W. A. Miller, Phys. Status Solidi A **49**, K31 (1978).
[56] M. Jergel and P. Mrafko, J. Non-Cryst. Solids **85**, 149 (1986).
[57] B. M. Darinskiĭ, Yu. E. Kalinin, and D. S. Saĭko, *Internal Friction in the Investigation of Metals, Alloys, and Nonmetallic Materials* [in Russian], Nauka, M., 1989, p. 3.
[58] Ya. I. Frenkel', *Introduction to the Theory of Metals* [in Russian], Nauka, Leningrad, 1972.

[59] B. M. Darinskiĭ, Yu. E. Kalinin, and D. S. Saiko, *Physics of Amorphous Alloys* [in Russian], Izhevsk, 1984, p. 77.
[60] P. H. Gaskell, Acta Metall. **29**, 1203 (1981).
[61] B. M. Darinskiĭ and Yu. E. Kalinin, in *Abstracts of Reports at the 8th All-Union Conference on the Glassy State*, Nauka, Leningrad, 1986, p. 173.
[62] T. Jagielinski and T. Egami, J. Appl. Phys. **55**, 1811 (1984).
[63] N. Morito and T. Egami, Acta Metall. **32**, 603 (1984).
[64] V. I. Lavrent'ev and V. A. Khonik, Metallofizika **10**, 95 (1988).
[65] G. V. Sidorova, A. A. Novikova, and G. A. Sirotina, *Amorphous Metal Materials* [in Russian], Izhevsk, 1988, p. 107.
[66] H. S. Chen, J. T. Krause, and E. Coleman, J. Non-Cryst. Solids **18**, 157 (1975).
[67] V. K. Leko and O. V. Mazurin, *Properties of Quartz Glass* [in Russian], Nauka, Leningrad, 1985.
[68] I. V. Zolotukhin, Fiz. Khim. Stekla **8**, 513 (1982).
[69] H. S. Chen, J. Appl. Phys. **49**, 3289 (1978).
[70] A. Inoue, H. S. Chen, J. T. Krause *et al.*, J. Mater. Sci. **18**, 2743 (1983).
[71] Yu. E. Kalinin and I. V. Zolotukhin, Fiz. Tverd. Tela **22**, 223 (1980) [Sov. Phys. Solid State **22**, 129 (1980)].
[72] H. U. Kunzi, K. Agueman, and H. T. Guntherodt, Solid State Commun. **32**, 711 (1979).
[73] H. N. Yoon and A. Eisenberg, J. Non-Cryst. Solids **29**, 357 (1978).
[74] I. V. Zolotukhin, A. S. Solov'ev, B. G. Sukhodolov, and Yu. V. Barmin, *Internal Friction in the Investigation of Metals, Alloys, and Nonmetallic Materials* [in Russian], Nauka, M., (1988), p. 130.
[75] B. S. Berry, W. C. Pritchet, and C. C. Tsuei, Phys. Rev. Lett. **41**, 410 (1976).
[76] B. S. Berry and W. C. Pritchet, Phys. Rev. B **24**, 2299 (1981).
[77] H. U. Kunzi, E. Armbruster, and K. Agyeman, *Conference Metonallic Glasses: Science and Technology*, Bidapest, 1981, Vol. 1, p. 107.
[78] B. S. Berry and W. C. Pritchet, Scripta Metall. **15**, 637 (1981).
[79] I. V. Zolotukhin, V. I. Belyavskii, and V. A. Khonik, Fiz. Tverd. Tela **27**, 1788 (1985) [Sov. Phys. Solid State **27**, 1072 (1985)].
[80] V. I. Belyavskiĭ, V. A. Khonik, and T. N. Ryabtseva, Metallofiz. **11**, 107, 1989.
[81] I. V. Zolotukhin, Yu. E. Kalinin, and V. I. Kirillov, *Physics and Chemistry of Glass* [in Russian], Metallurgiya, M., 1983, p. 97.
[82] I. V. Zolotukhin and Yu. E. Kalinin, Fiz. Khim. Stekla **7**, 3 (1981).
[83] Yu. V. Barmin, Yu. E. Kalinin, and I. A. Safonov, *New Materials for Electronics* [in Russian], Voronezh, 1983, p. 32.
[84] I. V. Zolotukhin, Yu. V. Barmin, and A. V. Sitnikov, Fiz. Tverd. Tela **25**, 3456 (1983) [Sov. Phys. Solid State **25**, 1988 (1983)].
[85] B. S. Berry, Scripta Metall. **16**, 1407 (1982).
[86] H. R. Sinning and F. Haessner, J. Non-Cryst. Solids **93**, 53 (1987).
[87] S. Tuargi and A. S. Lord, *ibid.* **30**, 273.
[88] H. R. Sinning and F. Haessner, Scripta Metall. **20**, 1541 (1986).
[89] T. Soshiroda, M. Koiwa, and T. Masumoto, J. Non-Cryst. Solids **22**, 173 (1976).
[90] I. V. Andreev, Yu. S. Balashov, and O. V. Mazurin, Fiz. Khim. Stekla **6**, 203 (1980).
[91] N. Morito, Mater. Sci. Eng. **60**, 261 (1983).
[92] N. Morito and T. Egami, IEEE Trans. Magn. **19**, 1898 (1983).
[93] N. Morito and T. Egami, *ibid.*, 1901.
[94] B. S. Berry, *Glassy Metals* [Russ. transl. Metallurgiya, M., 1984, p. 128].
[95] Yu. E. Kalinin, I. A. Safonov, and S. V. Tolstykh, *Amorphous Metal Materials* [in Russian], Izhevsk, 1988, No. 9, p. 50.
[96] V. S. Postnikov, Internal Friction in Metals [in Russian], Metallurgiya, M., 1974.
[97] A. S. Nowik and B. S. Berry, *Anelastic Relaxation in Crystalline Solids*, Academic Press, N. Y., 1972 [Russ. transl., Atomizdat, M., 1975].
[98] S. L. Revo, V. E. Badan, and V. S. Kopan', Metallofizika **8**, 6 (1986).
[99] A. I. Gubanov, Fiz. Tverd. Tela **2**, 502 (1960) [Sov. Phys. Solid State **2**, 468 (1960)].
[100] W. B. Grigsons, D. B. Dove, and G. R. Stelwell, Nature **204**, 173 (1964).
[101] I. B. Kekalo and V. Yu. Novikov, Progress in Science and Technology. Series on Metal Science and Heat Treatment [in Russian], VINITI, Academy of Sciences of the USSR, Moscow (1984), Vol. 18, p. 1.
[102] W. A. Hines, A. H. Menotti, J. I. Budnick *et al.*, Phys. Rev. B **13**, 4060 (1976).
[103] M. B. Stearns, *ibid.*, 1383.
[104] R. C. O'Handley, Appl. Phys. **62**, R15 (1987).
[105] T. Mizoguchi, T. R. McGuire, R. Gambino, and S. Kirkpatrick, Physica B **86–88**, 783 (1977).
[106] K. Handrich, Phys. Status Solidi B **32**, K55 (1969).
[107] R. P. Messmer, Phys. Rev. B **23**, 1616 (1981).
[108] B. W. Corb, R. C. O'Handley, and N. J. Grant, J. Appl. Phys. **53**, 7728 (1982).
[109] B. W. Corb and R. C. O'Handley, Phys. Rev. B **31**, 7213 (1985).
[110] S. L. Ginzburg, *Physics of the Condensed State* [in Russian], Leningrad Institute of Nuclear Physics of the Academy of Sciences of the USSR, Leningrad, 1982, p. 43.
[111] K. H. Fischer, Phys. Status Solidi B **116**, 357 (1983); **130**, 13 (1985).
[112] I. Ya. Korenblit and E. F. Shender, Izv. Vyssh. Uchebn. Zaved., Fiz., No. 10, 23 (1984) [Sov. Phys. J. **27**, 822 (1984)].
[113] K. Binder and A. P. Young, Rev. Mod. Phys. **58**, 801 (1986).
[114] C. Y. Huang, J. Magn. Magn. Mater. **51**, 1 (1985).
[115] H. Malentta and W. Zinn, Ber.Kernforschungsanlage, Julich, No. 2084, 1 (1986).
[116] S. L. Ginzburg, *Mechanisms of High-Temperature Superconductivity* [in Russian], Dubna, 1988, p. 107.
[117] R. K. Mikhoradhyay and A. K. Raychaudhuri, J. Phys. C **21**, L385 (1988).
[118] I. B. Kekalo, Progress in Science and Technology. Series on Metals Science and Heat Treatment, VINITI, Academy of Sciences of the USSR, M., 1973, Vol. 7, p. 5.
[119] I. V. Zolotukhin, Yu. E. Kalinin, I. B. Kekalo, and B. G. Sukhodolov, Metallofizika **6**, 58 (1984).
[120] N. P. Kobelev and Ya. M. Soifer, Fiz. Tverd. Tela **28**, 425 (1986) [Sov. Phys. Solid State **28**, 236 (1986)].
[121] K. I. Arai and N. Tsuya, Sci. Rep. Ser. A, RITU, **30**, Suppl. P. 247 (1980).
[122] K. Fukamuchi and T. Masumoto, IEEE. Trans. **MAG-15**, 1404 (1979).
[123] S. Ishio and M. Takahashi, J. Magn. Magn. Mater. **50**, 93 (1985).
[124] K. Handrich and S. Kobe, *Amorphous and Ferro- and Ferrimagnets* [Russ. transl., Mir, M., 1982.]
[125] S. A. Nikitin, I. V. Zolotukhin, A. S. Solov'ev *et al.*, Fiz. Tverd. Tela **29**, 1526 (1987) [Sov. Phys. Solid State **29**, 874 (1987)].
[126] N. S. Kazama, H. Fujimori, and K. Hirose, IEEE Trans. **MAG-18**, 1182 (1982).
[127] H. Sakakima, *ibid.* **MAG-19**, 131 (1983).
[128] H. Fujimori, N. S. Kazama, K. Hirose *et al.*, J. Appl. Phys. **55**, 1769 (1984).
[129] G. Balasubramanian, A. N. Tiwari, and C. M. Srivastava, J. Mater. Sci. Lett. 7, 1142 (1988).
[130] J. Gonzalez and E. du Tremolet de Lacheisserie, J. Magn. Magn. Mater. **78**, 237 (1989).
[131] G. Hausch and H. Warlimont, Z. Metallk. **64**, 152 (1973).
[132] M. Kikuchi, K. Fukamichi, T. Masumoto *et al.*, Phys. Status Solidi A **48**, 175 (1978).
[133] V. S. Postnikov, *Physics and Chemistry of Solids* [in Russian], Metallurgiya, Moscow (1978).
[134] I. V. Zolotukhin, Yu. E. Kalinin, and V. A. Kondusov, Pis'ma Zh. Tekh. Fiz. **14**, 339 (1988) [Sov. Tech. Phys. Lett. **14**, 149 (1988)].
[135] I. V. Zolotukhin, Yu. E. Kalinin, V. A. Kondusov, and B. G. Sukhodolov, Metallofizika **11**, 48 (1989).
[136] J. D. Livingston, Phys. Status Solidi A **70**, 591 (1982).
[137] I. V. Zolotukhin, Yu. E. Kalinin, and V. A. Kondusov, Fiz. Tverd. Tela **32**, 765 (1990) [Sov. Phys. Solid State **32**, 451 (1990)].
[138] B. S. Berry and W. C. Pritchet, Phys. Rev. Lett. **34**, 1022 (1975).
[139] M. A. Mitchell, J. R. Cullen, and R. Abbundi, J. Appl. Phys. **50**, 1627 (1979).
[140] M. Brouha and J. van der Borst, *ibid.*, 7594.
[141] N. P. Kobelev, Ya. M. Soifer, V. G. Shteinberg, and Yu. B. Levin, Fiz. Tverd. Tela **29**, 1564 (1987) [Sov. Phys. Solid State **29**, 898 (1987)].
[142] I. V. Zolotukhin, Yu. E. Kalinin, B. G. Sukhodolov, and I. A. Safonov, *Problems of the Investigation of the Structure of Amorphous Metallic Alloys* [in Russian], MISiS (Moscow Institute of Steel and Alloys), M., 1984, p. 179.
[143] Yu. E. Kalinin, B. G. Sukhodolov, I. V. Zolotukhin, and V. P. Alekhin, Fiz. Met. Metalloved. **55**, 243 (1983) [Phys. Met. Metallogr. (USSR) **55**(2), 29 (1983)].
[144] B. S. Berry and W. C. Pritchet, J. Appl. Phys. **47**, 3295 (1976).
[145] G. W. Smith and J. R. Birchak, *ibid.* **41**, 3315 (1970).
[146] V. I. Minakov and V. N. Fedosov, Fiz. Met. Metalloved. **60**, 412 (1985) [Phys. Met. Metallogr. (USSR) **60**(2), 195 (1985)].
[147] J. H. Perepezko and J. W. Wiley, "*Semiconductor device having an amorphous metalayer contact*," US Patent No. 4494136 (1985).
[148] Yu. V. Barmin, I. V. Zolotukhin, Yu. A. Obvintsev, and O. V. Stogneĭ, Inventor's Certificate No. 1464500, July 29, 1987.
[149] Yu. V. Barmin, I. V. Zolotukhin, V. V. Vavilova *et al.*, Dokl. Akad. Nauk SSSR **304**, 895 (1989) [Dokl. Phys. Chem. (1989)].
[150] K. Mohri, IEEE Trans. **MAG-20**, 942 (1984).
[151] V. A. Kondusov, *Author's Abstract of Candidate's Dissertation in Physical and Mathematical Sciences*, Voronezh, 1989.

Translated by M. E. Alferieff